

000 001 002 003 004 005 006 007 008 009 010 011 012 013 014 015 016 017 018 019 020 021 022 023 024 025 026 027 028 029 030 031 032 033 034 035 036 037 038 039 040 041 042 043 044 045 046 047 048 049 050 051 052 053 TATTOO: TOOL-GROUNDED THINKING PRM FOR TEST-TIME SCALING IN TABULAR REASONING

Anonymous authors

Paper under double-blind review

ABSTRACT

Process Reward Models (PRMs) have recently emerged as a powerful framework for enhancing the reasoning capabilities of large reasoning models (LRMs), particularly in the context of test-time scaling (TTS). However, their potential for supervising LRM on tabular reasoning domains remains underexplored. Through detailed empirical analyses, we identify that existing PRMs, though widely adopted for supervising text-only reasoning steps, struggle with table-specific operations such as sub-table retrieval and schema interaction, leading to critical performance bottlenecks. To address this limitation, we propose TATTOO, a novel table-grounded PRM framework that (i) reasons explicitly over tabular reasoning steps and (ii) integrates tool-based verification to provide precise reward supervision. Concretely, we first design a scalable data curation pipeline that constructs over 60k high-quality step-level annotations by integrating table verification rationales with tool-based executions. Building on the collected data, we train TATTOO with a dual-stage paradigm: cold-start supervised fine-tuning to capture tool-use reasoning patterns, followed by reinforcement learning with tool-grounded reward shaping to align our model with table-based verification. We provide a comprehensive evaluation of the policy improvement induced by our newly designed PRM. Across 5 challenging tabular reasoning benchmarks covering numerical reasoning, fact-checking, and data analysis, TATTOO improves downstream policy LRM by 30.9% at inference, surpasses strong PRM baselines such as Qwen-2.5-Math-PRM-72B with only 8B parameters, and demonstrates strong generalizability across diverse TTS strategies.

1 INTRODUCTION

Tabular reasoning has become a fundamental capability for emerging large reasoning models (LRMs) across various real-world applications, including numerical analysis (Akhtar et al., 2023; Sui et al., 2024), fact-checking (Chen et al., 2019; Parikh et al., 2020), and question answering (Vakulenko and Savenkov, 2017; Li et al., 2023a). Unlike free-form text, tables encode information in rows and columns with an implicit relational semi-structure. Effective reasoning over tables therefore requires both accurate interpretation of tabular content and step-by-step logical inference to produce precise answers (Wang et al., 2024c; Zhang et al., 2025a). To support such multi-step reasoning, recent studies such as Table-R1 series (Wu et al., 2025b; Yang et al., 2025b; Jin et al., 2025) have incorporated reinforcement learning (RL) techniques (Schulman et al., 2017; Shao et al., 2024) to better align LRM with the demands of complex table understanding and reasoning.

On the other hand, process reward models (PRMs) (Setlur et al., 2024; Wang et al., 2024b; Yang et al., 2024) have been developed to provide step-level supervision over model reasoning trajectories during test-time scaling (TTS), offering fine-grained verification that enhances LRM's performance at inference. However, despite growing computational budgets and increasing emphasis on advancing LRM's tabular reasoning abilities (Ye et al., 2025; Muennighoff et al., 2025), a corresponding step-level PRM to supervise the reasoning quality of these models in table domains is equally important but remains notably absent. This gap motivates our study of a fundamental question:



How can we provide reliable step-level supervision to advanced LRM in tabular reasoning?

To investigate this question, we first revisit several general-domain advanced PRMs and evaluate their effectiveness in supervising table-involved reasoning steps generated by LRM. Our analysis reveals that existing PRMs struggle to reliably verify two critical types of tabular CoT steps: ① *Table Retrieval*, where PRMs fail to supervise whether LRM extract the correct sub-region of the input table relevant to the query; and ② *Schema Interaction*, where PRMs cannot detect attention collapse (Dong et al., 2021), as LRM often overlook long-range table dependencies due to inherent locality bias. Beyond challenges arising from the tabular input modality, we also observe that current PRMs frequently introduce supervision errors within their own evaluation process, stemming from inaccurate table lookups or failed operations on tables. These shortcomings amplify bias and noise during TTS, ultimately creating persistent performance bottlenecks.

Motivated by our preliminary analyses, we propose **TATTOO**, a new **Table Thinking PRM with Tool** integration abilities to provide more reliable and precise supervision for tabular reasoning. Distinct from prior PRMs that provide weak supervision over table-specific operations, TATTOO provides step-level supervision tailored to different input steps, applying both table-grounded rewards for tabular operation steps and inner-reasoning rewards for text-based reasoning steps. In addition, TATTOO can leverage several external tools to interact with table contents, execute code-based operations, and incorporate the results back into the step-by-step verification process. To build TATTOO, we first design a scalable data curation pipeline that yields over 60k high-quality supervision instances by integrating expert verification rationales with tool-based executions. We then train our PRM under a dual-stage paradigm: supervised fine-tuning to capture step-level tool-use reasoning patterns, followed by reinforcement learning with a newly designed reward shaping scheme to encourage effective tool manipulation and faithful reasoning for accurate verification. Finally, we provide theoretical intuition on the policy improvement induced by incorporating TATTOO during inference.

To demonstrate the effectiveness of TATTOO, we conduct extensive experiments on five challenging tabular reasoning benchmarks, covering table-based question answering, numerical reasoning, fact-checking, and data analysis. Across all benchmarks, incorporating 8B-size TATTOO improves downstream policy models by 30.9%. In addition, TATTOO consistently outperforms strong PRM baselines such as Qwen-2.5-Math-PRM-72B (Zhang et al., 2025b) and GenPRM-32B (Zhao et al., 2025) with up to 9x parameter efficiency. In-depth analyses further demonstrate that incorporating our dual-stage training paradigm yields a 10.2% improvement over standard PRM training, and TATTOO exhibits strong generalizability across diverse TTS strategies, including Beam Search and DVTS.

2 PRELIMINARY

Table Understanding with LRM. We denote $T = (H, R)$ as a semi-structured table, where H is the set of column headers defining the schema-level semantics, and R is the set of rows, with each row composed of cell entries aligned with H . Given a table T and an associated natural language query q , we define a reasoning model as a conditional generation policy $\pi(\tau | T, q)$, where $\tau = \{a_1, \dots, a_L\}$. Here, τ denotes the reasoning model’s generated reasoning trajectory, including both intermediate reasoning steps $\{a_i\}_{i=1}^{L-1}$ and the final answer a_L . In our problem setup, the intermediate reasoning steps consist of both model inner-thinking reasoning traces and tool-integrated programs that operate directly on the table to retrieve or compute intermediate results. The final answer can take different formats depending on the query type, including textual or numerical values, boolean outputs (e.g., True/False), or executable programs (e.g., Python, SQL).

Reward Modeling for Tabular Reasoning. Given a table T , a query q , and a candidate response τ generated by a policy LRM, a standard step-level verifier (i.e., PRM) parameterized by θ computes a scoring function $\mathcal{R}_\theta(\cdot)$ that assigns step-level rewards r_i evaluating the correctness of each step $a_i \in \tau$. The trajectory-level reward r_τ for each response τ is then obtained by aggregating these step-level rewards. Formally, we have:

$$r_i = \mathcal{R}_\theta(a_i | T, q, \tau_{<i}), \quad \text{with } r_\tau = \mathcal{A}(r_1, r_2, \dots, r_L), \quad (1)$$

where $\mathcal{A}(\cdot)$ denotes an aggregation function such as MEAN and SUM (Liu et al., 2025). The rewards provided by the PRM \mathcal{R}_θ can be further leveraged by a test-time compute strategy ϕ (e.g., Best-of-N (Brown et al., 2024), Beam Search (Snell et al., 2024)) to guide resampling, refinement, and candidate selection among the responses generated by the policy model.

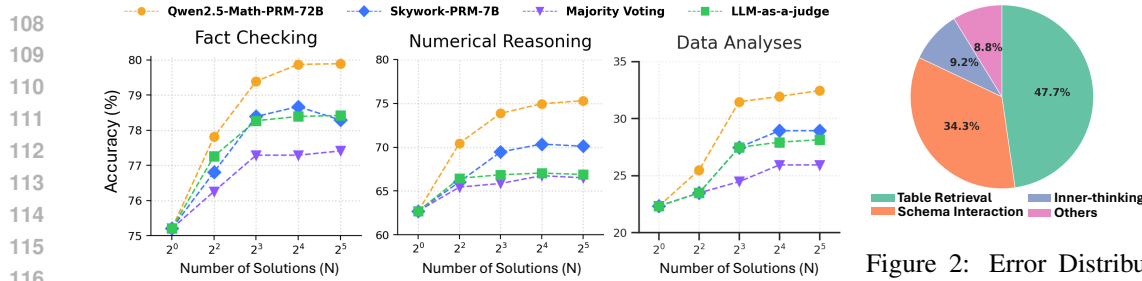


Figure 1: Best-of-N performance of DeepSeek-R1-Distill-Qwen-14B across 3 table tasks on TableBench with different types of step verifiers.

Figure 2: Error Distribution over 4 step categories across 500 incorrect cases after Best-of-N selection.

3 WHY TABLE REASONING REQUIRES VERIFIERS BEYOND CURRENT PRMs?

We begin by revisiting existing general-domain PRM methods to assess their effectiveness in supervising LRM s on tabular reasoning tasks and to identify potential performance bottlenecks. To this end, we conduct a pilot study guided by two key questions:

RQ1 - Beyond free-form text inputs, can common general-domain PRMs combined with TTS strategies also enhance the performance of LRM s on tabular reasoning tasks?

RQ2 - When step-level reward supervision is crucial for tabular reasoning performance, how can PRMs effectively supervise and guide the quality of each reasoning step generated by LRM s?

For brevity, we defer detailed experimental setups to Appendix F. To investigate RQ1, we evaluate various step-level verification methods, including two advanced PRMs (Qwen2.5-Math-PRM-72B (Zhang et al., 2025b) and Skywork-PRM-7B (He et al., 2024a)), majority voting (Liu et al., 2025), and LLM-as-a-judge (Zheng et al., 2023) with the Best-of-N TTS strategy. We choose DeepSeek-R1-Distill-Qwen-14B (Guo et al., 2025) as the common LRM and evaluate on TableBench (Wu et al., 2024), which includes three fundamental table tasks (Fact Checking, Numerical Reasoning, and Data Analysis). As shown in Figure 1, we observe that for small values of N , incorporating step-level verifiers into Best-of- N generally improves LRM s performance over single-shot generation, with PRMs providing the largest gains. However, once the number surpasses a threshold ($N \geq 8$), accuracy across all three table tasks converges to a bottleneck. For example, the performance of Qwen2.5-Math-PRM-72B on fact-checking is 79.19%, 79.82%, and 79.84% for $N = \{8, 16, 32\}$, indicating that further increases in N yield negligible gains, even though with PRM incorporation.

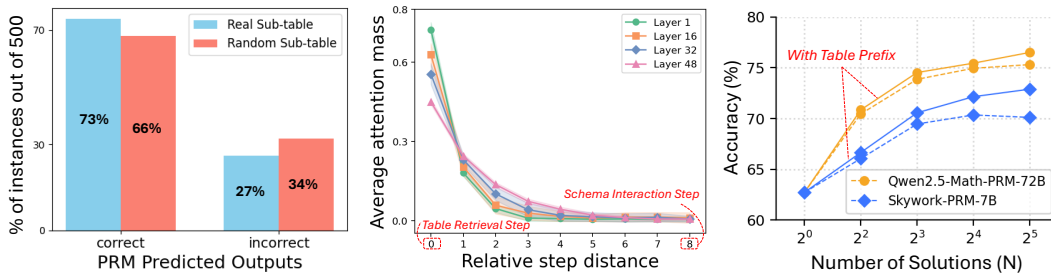
Observation 1 (Limitation on TTS): Existing PRMs yield modest improvements on tabular reasoning, but their efficacy quickly saturates, failing to fully exploit additional test-time compute.

Error Analysis. Building on the observation, we further investigate the underlying causes of the performance bottleneck by conducting an error analysis on LRM s generation and PRM s supervision processes. Specifically, we sample 500 erroneous Best-of-N responses ($N = 32$) selected by the PRM from LRM s outputs, and ask human experts to classify them into 13 well-defined tabular error types (see Appendix C). We then connect these errors with 4 reasoning-step categories reflecting the typical flow of LRM s reasoning process: (i) *Table Retrieval Steps*, locating relevant rows/columns regarding the input query; (ii) *Schema Interaction Steps*, reasoning over the retrieved table contents, (iii) *Inner-thinking Steps*, models inner reasoning independent of table contents, and (iv) *Others*, initial setup or final output steps that are irrelevant to core reasoning process. Figure 2 presents the error distribution across 4 reasoning step categories. We find that most errors arise in *Table Retrieval* (47.7%) and *Schema Interaction* (34.3%), implying that PRMs perform reasonably well on independent reasoning but fall short when reasoning steps involve table-specific operations. For better demonstration, we provide representative examples for each category in Table 1.

Why do PRMs fail on table-involved reasoning steps? Next, we take a closer look at why PRMs lose their supervisory effectiveness when reasoning steps involve table operations. For *Table Retrieval Steps*, we conduct a contrastive experiment focusing particularly on the table contents retrieved by LRM s within their responses. We randomly sampled 500 responses and constructed two variants by (i) retaining the original LRM-retrieved sub-table, and (ii) replacing it with a randomly selected sub-table region from the original input table. Figure 3 (left) shows the output rewards of Qwen2.5-Math-PRM-

162
163
164
165
166 Table 1: Representative error cases in 3 different reasoning step categories. Each example highlights
167 the erroneous model step in **red**, the corresponding error description, and the PRM’s (mis)judgment
168 reward, illustrating where existing PRMs fail to detect mistakes.
169
170
171

Category	Wrong Model Answer	Error Description & PRM output
Table Retrieval	<p><think> Step 1: I need to figure out the average prominence of mountain peaks in the Democratic Republic of the Congo that have an elevation of at least 3000 meters.</p> <p>Step 2: First, I'll review the provided table. My main focus is on the 'country' and 'elevation (m)' columns. (Wrong Step)</p> <p>...</think></p> <p>Final Answer is \boxed{2306.65}</p>	<p>The model initially retrieves the wrong part of the table (columns ‘Country’ and ‘Elevation (m)’), which leads to errors in all subsequent reasoning steps.</p> <p>PRM → {correct} ✗ Fail to detect the error</p>
Schema Interaction	<p><think> Step 1: Let me start by looking at the table provided ... The retrieved columns are ...</p> <p>Step 4: I'll go through each row and note down the episodes: Episode 1: Rating - 5.1, Episode 2: Rating - 5.2 ... (Wrong Step)</p> <p>Step 5: Adding the rating together is $5.1 + 5.2 + \dots$</think></p> <p>Final Answer is: \boxed{11.52}</p>	<p>The model identifies the correct column for the answer, but fails to extract all elements, omitting the last cell. This omission leads to incorrect reasoning in all subsequent steps.</p> <p>PRM → {correct} ✗ Fail to detect the error</p>
Inner-thinking	<p><think> Step 1: Based on the table contents, I need to count podiums per season. 2008: $(1 + 1 + 1)/3 = 1$, 2009: 6, 2010: 0, 2011: $(2 + 0)/2 = 1 \dots$</p> <p>Step 4: Then I will average across seasons. Final average is $(1 + 6 + 0 + 1)/4 = 2$ (Wrong Step)</p> <p></think></p> <p>Final Answer is: \boxed{2}</p>	<p>The model incorrectly does the calculation by averaging the season-level means, giving each season equal weight, instead of averaging across all team-seasons.</p> <p>PRM → {incorrect} ✓ Detect the error</p>



181
182
183
184
185
186
187
188
189
190
191 Figure 3: **Left:** PRM’s rewards on 500 reasoning steps with the real-retrieved/randomly-replaced
192 sub-table. **Middle:** Layer-wise average attention mass vs. relative step distance in tabular reasoning.
193 Attention concentrates on nearby steps, with sharp decay as distance increases. **Right:** Best-of-N
194 results on DeepSeek-R1-Distill-Qwen-14B for numerical reasoning with/without the table prefix.

195 72B on both variants. The nearly identical distributions between real and random sub-tables indicate
196 that current PRMs fail to distinguish retrieval correctness, suggesting that they are unable to assess
197 whether the LRM’s retrieved portion of the table corresponds to the query.

198
199 **Takeaway 1 (Table Retrieval):** Existing PRMs are insensitive to table retrieval correctness in
200 the reasoning steps and fail to recognize whether the retrieved content corresponds to the query.

201 For *Schema Interaction Steps*, we found in prior experiments that in the logic flow of LRM’s
202 trajectories, table retrieval steps typically occur at the beginning, as the model must first extract
203 relevant information from the table to answer the query. In contrast, schema interaction steps
204 frequently occur far sentences from the beginning table retrieval steps, since LRM’s tend to perform
205 intermediate reasoning before revisiting their retrieved contents when needed. Figure 3 (middle)
206 illustrates the attention distribution of the LRM between the schema interaction step (step 8) and
207 the table retrieval step (step 0). Due to the auto-regressive nature of LRM’s, the schema interaction
208 step attends primarily to nearby steps while assigning little attention to the earlier retrieval step. This
209 inherent locality bias causes the model to frequently misinterpret or discard previously retrieved
210 contents, even when the retrieval step has already extracted the correct information. Moreover, current
211 PRMs fail to supervise such misinterpretations, as their evaluations are highly localized to the current
212 step rather than capturing dependencies on distant prior steps (Zou et al., 2025; Feng et al., 2025b).

213
214 **Takeaway 2 (Schema Interaction):** Schema interaction steps under-attend to distant table
215 retrieval contents due to locality bias. PRMs miss these failures since they can’t look ahead and
capture long-range dependencies among distant steps.

216 **Table Prefix is the Key.** To explore potential solutions to the limitation above, we begin with a
 217 simple input modification for PRMs: prepending the retrieved table contents as a prefix to each
 218 schema interaction step. This grants PRMs direct access to the retrieval context, alleviating the need
 219 for long-range dependencies. We evaluate this modification and report the results in Figure 3 (right).
 220 Incorporating the table prefix indeed improves PRM supervision and leads to stronger downstream
 221 LRM performance. However, directly applying the prefix remains challenging, as current PRMs
 222 cannot automatically identify schema interaction steps, and the table prefixes obtained from LRMs
 223 are not guaranteed to be correct without proper supervision.

224 **Motivation for TATTOO.** Our analyses above highlight the need for a principled step-level verifier
 225 capable of providing robust supervision over both table-grounded operations and models’ inner
 226 reasoning. Motivated by this, we propose a new process reward model specifically designed to
 227 support LRMs in tabular reasoning.

228 4 BUILDING A TABLE-GROUNDED STEP VERIFIER

230 We introduce TATTOO, a generative PRM that provides reward supervision over both table operations
 231 and model inner thinking steps. Our method builds on two key components: (i) a large-scale data
 232 curation pipeline that synthesizes reasoning and tool usage for PRM training, and (ii) a dual-stage
 233 training paradigm that learns step-level verification with tool use optimization.

234 4.1 TABLE-AWARE AND TOOL-INTEGRATED SUPERVISION

236 **Table-Aware Reward.** To align with the LRM’s reasoning process on table tasks, we separate
 237 the supervision of table operations from model’s inner reasoning part and decompose TATTOO’s
 238 step-level reward (Eq. 1) into two components:

$$240 \quad r_i = \begin{cases} r_{i,\text{rea}}, & \text{if } a_i \in \text{inner-thinking}, \\ r_{i,\text{tab}}, & \text{if } a_i \in \text{table retrieval or schema interaction}, \end{cases} \quad \text{and } r_\tau = \frac{1}{L} \sum_{i=1}^L r_i, \quad (2)$$

243 where $r_{i,\text{rea}}$ captures the correctness of the model inner-reasoning process, $r_{i,\text{tab}}$ reflects the accuracy
 244 of table-grounded operations, and r_τ denotes the trajectory-level reward.

245 **Tool Integration in Verification.** A major limitation of current PRMs is their inability to supervise
 246 table-involved reasoning steps (as shown in Section 3). Meanwhile, recent studies (Feng et al.,
 247 2025a; Qian et al., 2025) have shown that LLM agents can autonomously use **tools** to interact with
 248 external environments and iteratively refine their reasoning. In a similar spirit to address current
 249 PRM’s limitation, we incorporate several external table-oriented tools into TATTOO’s verification
 250 process to enable more reliable step supervision. We next describe how we curate a training set with
 251 tool-augmented, table-aware rewards and use it to train TATTOO.

252 4.2 TATTOO DATA CURATION PIPELINE

254 We design a large-scale data curation pipeline that simulates real-world scenarios of PRM tool use
 255 and step verification at scale. As illustrated in Figure 4, there are three main stages:

256 **1 Reasoning Trajectory Generation.** We begin by collecting trajectory responses from expert
 257 LRM (e.g., DeepSeek-R1 (Guo et al., 2025) and Claude-Opus-4.1 (Anthropic, 2025)) on table-based
 258 questions drawn from diverse benchmarks, including TableInstruct (Wu et al., 2024), HybridQA (Chen
 259 et al., 2020), ToTTo (Parikh et al., 2020), and WikiTQ (Pasupat and Liang, 2015b). We generate
 260 multiple responses per query and apply dual verification with human annotators and expert LLMs to
 261 filter out low-quality data, yielding a high-quality trajectory pool $\mathcal{T}_{\text{pool}}$ for subsequent labeling.

262 **2 Verification Synthesis & Reward Assignment.** We next provide step-level verification rationales
 263 and reward labels for each candidate response in $\mathcal{T}_{\text{pool}}$. (i) For *table retrieval steps*, we extract the
 264 sub-table in each step and use LLM-as-a-judge to assess its relevance to the query, assigning table
 265 reward $r_{i,\text{tab}} \in \{-1, 1\}$ based on retrieval correctness. (ii) For *schema interaction steps*, we prepend
 266 the accurate sub-table as a table prefix to each collected verification rationale (according to our
 267 table-prefix analysis in Section 3) and assign $r_{i,\text{tab}} \in \{-1, 1\}$ based on the correctness of the specific
 268 table-based operations or reasoning. (iii) For *inner-thinking steps*, which involve no table contents,
 269 we apply LLM-as-a-judge and follow established labeling strategies (Zhao et al., 2025; Khalifa et al.,
 270 2025) to assign $r_{i,\text{rea}} \in \{-1, 1\}$ based on reasoning quality.

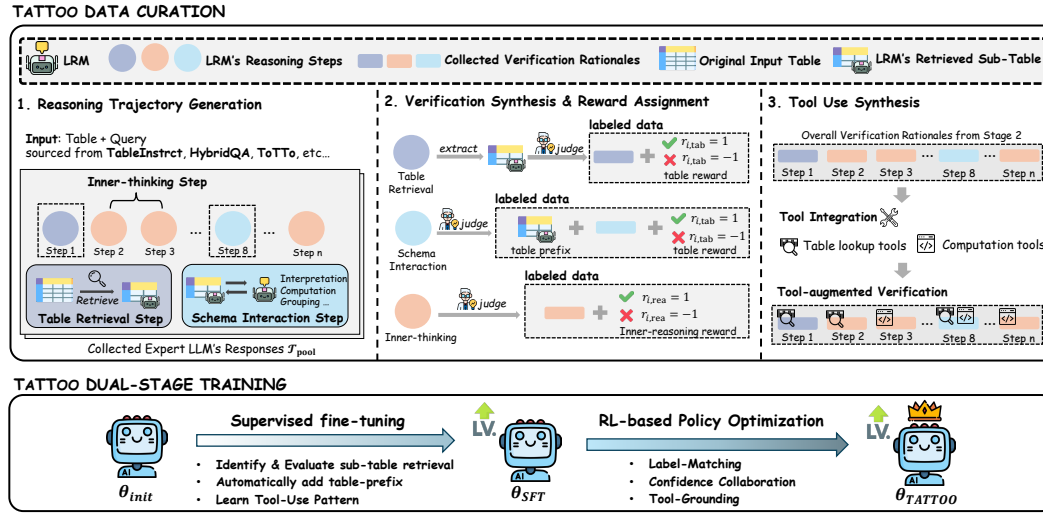


Figure 4: **Overview of TATTOO framework.** We first curate 60k high-quality instances by collecting expert verification rationales with tool integration (Section 4.2). We then train our PRM through a dual-stage training paradigm to achieve tool-grounded step-by-step reward supervision (Section 4.3).

3 Tool Use Synthesis. To train TATTOO to leverage tools for more accurate verification, we further augment the collected verification rationales with tool invocations, execution results, and feedback at the step level. Specifically, inside the rationale contents, we replace manual reasoning for table lookups or calculations with the corresponding tool call and its execution output. We primarily employ two types of table tools: (i) *Computation tools*: code snippets (e.g., Python, SQL) for arithmetic and aggregation over table inputs; (ii) *Table Lookup tools*: DataFrame APIs (e.g., Polars) or Lookup Utilities (e.g., CSV/Excel readers) for retrieving specific rows, columns, or cells during verification.

Finally, we construct over 60k high-quality training instances with complete verification rationales and step-level rewards. This dataset is then used to train TATTOO to integrate tool use with reasoning for robust step supervision. We leave additional data curation details in Appendix D.

4.3 TOOL-GROUNDED DUAL-STAGE TRAINING

With the training data recipe in place, we train TATTOO via a dual-stage paradigm: supervised fine-tuning to capture tool-integrated verification patterns, followed by RL-based policy optimization with a newly designed reward shaping scheme to further refine our PRM’s step-level rationales and ensure accurate verification.

Table-Aware Verification with Tools via SFT. We first finetune our PRM \mathcal{R}_θ on the curated dataset (Section 4.2). Specifically, given a training instance (T, q, τ) consisting of a table T , a query q , and an LRM-generated trajectory $\tau = (a_1, \dots, a_L)$, we train the PRM to output, for each step $a_i \in \tau$, a verification rationale v_i together with its corresponding step-level reward r_i . By formulating PRM training as language modeling, \mathcal{R}_θ is optimized auto-regressively to (i) identify accurate sub-table regions, (ii) learn to dynamically incorporate the retrieved table prefix into each schema interaction step, and (iii) generate verification rationales with tool-integration patterns.

Tool-Grounded Reward Shaping in RL. Prior generative PRM approaches (Liu et al., 2025; Khalifa et al., 2025; Zhao et al., 2025) typically conclude PRM training after the SFT stage. In contrast, we draw inspiration from recent advances in agentic RL (Jaech et al., 2024; Guo et al., 2025) and further apply policy optimization to more tightly align the PRM’s verification process with effective tool utilization. Specifically, we optimize \mathcal{R}_θ with a modified GRPO (Shao et al., 2024) by providing dense, tool-grounded supervision signals during policy optimization. During RL rollouts of each training instance (T, q, τ) , we replace the original rule-based GRPO supervision signal with a denser per-step reward signal s_i , defined as:

$$s_i = \underbrace{\mathbb{1}\{\hat{r}_i = r_i\}}_{\text{label-matching}} - \underbrace{\lambda_{\text{cal}} \left(-\log \mathcal{R}_\theta(r_i | T, q, \tau) \right)}_{\text{confidence calibration}} + \underbrace{\lambda_{\text{tool}} \cdot \text{support}(\hat{v}_i)}_{\text{tool-grounding}}, \quad (3)$$

where \hat{r}_i is the PRM’s predicted step-reward and r_i is the ground-truth step-reward for the input step $a_i \in \tau$; \hat{v}_i denotes the verification rationale generated by the PRM at step i , and $\text{support}(\hat{v}_i) \in \{0, 1\}$

measures whether the rationale correctly incorporates tool outputs; and λ_{cal} , λ_{tool} are tunable coefficients. Besides enforcing correctness with the *label-matching term*, the *confidence calibration term* stabilizes training by encouraging higher probability on the ground-truth label, and the *tool-grounding term* encourages rationales that effectively incorporate tool outputs.

The tool-grounding term encourages the PRM to incorporate correct tool-execution outputs into the generated verification rationale. Specifically, $\text{support}(\cdot)$ evaluates whether the rationale contains and correctly leverages executed tool results. When a tool call fails during an RL rollout, $\text{support}(\cdot)$ is automatically set to 0, and the error message is fed back into the model’s context. This prevents the PRM from reinforcing erroneous tool-based reasoning and trains it to down-weight steps associated with unstable or invalid tool calls.

We then aggregate the per-step signals s_i into a trajectory-level training reward, normalize it within each sampled group to compute group-relative advantages, and update the PRM \mathcal{R}_θ under the GRPO objective.

4.4 INFERENCE-TIME POLICY IMPROVEMENT – AN INTUITIVE VIEW

To intuitively elucidate the role of TATTOO and its table-aware rewards on LRM’s tabular reasoning process (Eq. 2), we provide a theoretical analysis on the policy improvement induced by TATTOO.

Recall that the goal of our PRM is to improve the generated trajectory τ sampled from a policy LRM π , i.e., $\tau \sim \pi(\cdot | T, q)$. By combining the input table and query, we represent $(T, q, a_1, \dots, a_{i-1})$ as the current state s_i . At step i , the policy LRM π samples an action $a_i \sim \pi(\cdot | s_i)$. We define the Q -value of policy π as the expected future success, measured by the final answer a_L correctness, i.e.,

$$Q^\pi(s_i, a_i) = Q^\pi((T, q, a_1, \dots, a_{i-1}), a_i) = \mathbb{E}_{a_{i+1}, \dots, a_L \sim \pi(\cdot | s_i)} [\mathbb{1}_{a_L \text{ is correct}}]. \quad (4)$$

The value of policy π at state s_i is defined as the expectation of Q -values under π ’s next action distribution: $V^\pi(s_i) = \mathbb{E}_{a_i \sim \pi(\cdot | s_i)} [Q^\pi(s_i, a_i)]$. We now analyze the policy improvement afforded by TATTOO’s table-aware reward r_i supervision under one step of a natural policy gradient updating.

Theorem 4.1 (Policy Improvement (Lower Bound)). *Given the current policy π , after one natural policy gradient update step guided by the PRM reward r_i defined in Eq. 2, we obtain the revised policy $\pi'(a_i | s_i) \propto \exp(Q^\pi(s_i, a_i) + r_i(s_i, a_i))$. The resulting expected policy improvement over the state distribution ρ then satisfies:*

$$\begin{aligned} \mathbb{E}_{s_i \sim \rho} [V^{\pi'}(s_i) - V^\pi(s_i)] &\gtrsim \underbrace{\mathbb{E}_{s_i \sim \rho} \text{Var}_{a_i \sim \pi(\cdot | s_i)} [r_{i, \text{tab}}(s_i, a_i)]}_{\text{distinguishability from table reward } r_{i, \text{tab}}} + \underbrace{\mathbb{E}_{s_i \sim \rho} \text{Var}_{a_i \sim \pi(\cdot | s_i)} [r_{i, \text{rea}}(s_i, a_i)]}_{\text{distinguishability from inner-reasoning reward } r_{i, \text{rea}}} \\ &\quad + \underbrace{\mathbb{E}_{s_i \sim \rho} \mathbb{E}_{a_i \sim \pi(\cdot | s_i)} [r_{i, \text{tab}}(s_i, a_i) A^\pi(s_i, a_i)]}_{\text{alignment between } r_{i, \text{tab}} \text{ and } A^\pi} + \underbrace{\mathbb{E}_{s_i \sim \rho} \mathbb{E}_{a_i \sim \pi(\cdot | s_i)} [r_{i, \text{rea}}(s_i, a_i) A^\pi(s_i, a_i)]}_{\text{alignment between } r_{i, \text{rea}} \text{ and } A^\pi}, \end{aligned} \quad (5)$$

where $A^\pi(s_i, a_i) = Q^\pi(s_i, a_i) - V^\pi(s_i)$ denotes the advantage of policy π .

Theorem 4.1 (proof in Appendix E) explains that our decomposable reward design r_i enables each component to additively contribute to policy improvement, provided that the reward components are each individually aligned with the policy advantage function. In this way, the table-aware rewards provided by TATTOO help ensure targeted supervision on both inner reasoning and table-involved operations generated by LRMs. Below, we further empirically evaluate the effectiveness of TATTOO across various downstream tabular reasoning tasks.

5 EMPIRICAL EVALUATIONS

Baselines and Models. We compare TATTOO against various types of step-level verification methods, including advanced PRMs, majority voting (Liu et al., 2025), and LLM-as-a-judge (Zheng et al., 2023). The setups for these baselines are aligned with our preliminary analyses in Section 3. For PRM approaches, we include both discriminative (Qwen-PRM series (Zhang et al., 2025b), Math-Shepherd-PRM (Wang et al., 2024b), and Skywork-PRM (He et al., 2024a)) and generative (ThinkPRM (Khalifa et al., 2025) and GenPRM (Zhao et al., 2025)). Regarding the policy reasoning models, we evaluate

378 Table 2: Main results of TATTOO on 5 different tabular reasoning tasks. We report the best-of-N
379 (with $N = \{4, 8, 16, 32\}$) performance using DeepSeek-R1-Distill-Qwen-14B as the policy model
380 and compare against various step verifiers. The best and second-best results are highlighted. TATTOO
381 consistently achieves state-of-the-art TTS performance with significantly fewer parameters.

Verifier (Best-of-N)	Params	TB-NR				TB-FC				TB-DA				WTQ				MMQA			
		4	8	16	32	4	8	16	32	4	8	16	32	4	8	16	32	4	8	16	32
Majority Vote	-	65.5	65.9	66.8	66.5	76.2	77.3	77.3	77.4	23.5	24.5	26.0	26.1	64.7	65.3	67.3	67.0	18.4	19.4	20.4	20.1
LLM-as-a-judge	-	66.7	66.9	67.1	66.9	77.2	78.3	78.4	78.6	23.5	27.4	28.0	28.4	65.2	66.4	68.1	68.1	19.6	21.3	22.5	22.7
Skywork-PRM-7B	7B	66.1	69.5	70.3	70.1	76.8	78.4	78.6	78.3	24.1	27.5	28.9	29.1	65.9	67.5	68.4	68.6	21.4	24.6	25.1	25.3
Math-Shepherd-PRM-7B	7B	67.2	70.6	71.5	71.8	76.2	76.9	76.8	77.1	22.7	24.8	26.4	25.9	66.8	68.7	69.6	69.3	22.0	25.2	25.9	26.1
Qwen2.5-Math-PRM-7B	7B	66.9	70.1	71.7	72.5	75.4	77.2	77.9	77.4	23.2	25.4	26.3	26.6	65.2	68.5	69.6	69.7	23.5	25.2	27.1	27.3
ThinkPRM	14B	69.2	70.7	73.5	73.8	75.8	75.4	76.3	76.9	21.6	22.7	23.1	22.8	64.3	66.1	65.7	65.9	22.4	22.7	23.6	23.0
GenPRM	32B	71.5	73.5	73.7	74.2	76.3	78.5	79.2	79.4	25.3	27.9	30.2	30.7	69.8	72.5	73.3	73.1	23.8	25.4	26.2	26.4
Qwen2.5-Math-PRM-72B	72B	70.4	73.8	74.9	75.3	77.8	79.2	79.8	79.8	25.5	31.5	32.0	32.4	69.2	71.8	73.0	72.6	24.4	26.8	28.7	28.6
TATTOO	8B	71.2	74.2	76.4	78.1	77.4	79.6	81.2	82.0	27.7	31.9	33.6	34.3	69.8	72.3	73.5	74.9	25.1	27.2	29.1	30.5

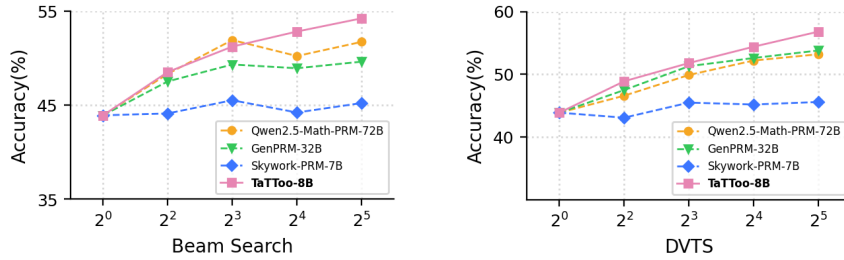
391
392 our proposed method on DeepSeek-R1-Distill-Qwen-14B (Guo et al., 2025). Further details on the
393 baselines and policy models setups are provided in Appendix F.1.

394
395 **Datasets.** We evaluate on four representative and challenging benchmarks spanning diverse tabular
396 reasoning tasks, including (i) TableBench (TB) (Wu et al., 2024), a complex tabular reasoning
397 benchmark with 886 questions covering tasks of numerical reasoning (NR), fact checking (FC),
398 and data analysis (DA). (ii) WTQ (Pasupat and Liang, 2015b), a benchmark for complex question
399 answering over Wikipedia tables. (iii) MMQA (Wu et al., 2025a), a multi-table understanding
400 benchmark covering table retrieval, multi-hop & multi-table QA and text-to-SQL generation. We
401 leave the additional dataset descriptions in Appendix F.2.

402
403 **Implementation Details.** We train TATTOO on the off-the-shelf Qwen-3-8B model (Yang et al.,
404 2025a) using our 60k curated training instances (Section 4.2). All training and inference experiments
405 are conducted on 8xA100-80G GPUs. To evaluate TATTOO under different TTS strategies, we adopt
406 three representative methods, including Best-of-N (Brown et al., 2024), Beam Search (Snell et al.,
407 2024), and Diverse Verifier Tree Search (DVTS) (Beeching et al., 2024). Additional implementation
408 details on training setup and configurations of TATTOO are provided in Appendix F.3.

5.1 MAIN RESULTS

410
411 Table 2 reports the Best-of-N performance of incorporating TATTOO on the DeepSeek-R1-Distill-
412 Qwen-14B model across five tabular reasoning tasks. Notably, TATTOO consistently outperforms
413 strong baselines such as GenPRM-32B and Qwen2.5-Math-PRM-72B despite using only 8B pa-
414 rameters. On TB-DA, TATTOO achieves the largest accuracy performance across each level of N,
415 rising from 27.7% at N=4 to 34.3% at N=32. Moreover, while existing PRMs often suffer from
416 performance bottlenecks beyond a certain response threshold (as observed in Section 3), TATTOO
417 continues to scale effectively, yielding consistent gains as the response group size increases. For
418 example, on TB-NR, Qwen2.5-Math-PRM-72B saturates after N=16 (74.9% \rightarrow 75.3%), whereas
419 TATTOO continues to improve from 74.2% at N=8 to 78.1% at N=32. These results demonstrate that
420 TATTOO provides stronger reward supervision on LRM’s reasoning trajectories, therefore yielding
421 better performance improvement compared with other step-verification baselines.



431 Figure 5: Performance of TATTOO on two additional TTS strategies, Beam Search and Diverse
432 Verifier Tree Search (DVTS). We report the average accuracy across all 5 tabular reasoning tasks.

432
 433 Table 3: In-depth analysis of TATTOO on three table datasets. We evaluate the contributions of SFT
 434 and RL training stages, and assess the impact of reward shaping components during RL optimization.

435 436 Training Variants	437 TB-NR				438 TB-FC				439 TB-DA			
	4	8	16	32	4	8	16	32	4	8	16	32
TATTOO (SFT only)	67.9	69.1	72.0	73.7	71.5	73.0	74.6	75.2	23.3	25.6	26.2	26.4
TATTOO	71.2	74.2	76.4	78.1	77.4	79.6	81.2	82.0	27.7	31.9	33.6	34.3
w/o tool-grounding	68.5	71.1	72.7	74.6	73.2	75.6	75.5	76.3	26.2	28.1	28.7	30.3
w/o confidence calibration	71.1	73.7	74.3	76.2	76.4	76.7	78.4	80.5	27.4	29.5	31.3	33.2
rule-based (GRPO)	67.0	68.4	70.4	73.1	71.6	74.0	74.9	75.8	25.5	27.4	28.0	28.6

442
 443 **Generalizability on Other TTS Strategies.** Beyond best-of- N , we also evaluate TATTOO under two
 444 additional TTS strategies (Beam Search and DVTS) and compare with the strongest PRM baselines.
 445 Figure 5 reports the average performance across the five tabular reasoning tasks. Under each TTS
 446 strategy, TATTOO consistently yields steady improvements as the number of responses N increases,
 447 whereas other baseline PRMs often plateau. For example, in beam search, TATTOO improves from
 448 45.0% to 54.8%, while GenPRM saturates around 51% and Skywork-PRM remains below 46%.
 449 These results highlight the strong generalizability of TATTOO across diverse TTS strategies.

450 5.2 IN-DEPTH ANALYSES ON TATTOO

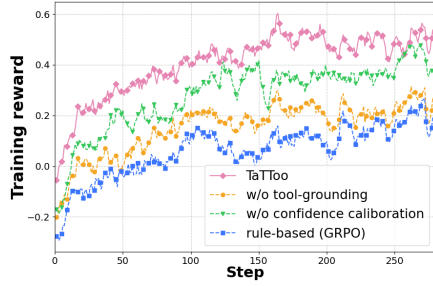
451 **Mastery of RL with Bootstrapping from SFT.** To examine the respective roles of SFT and RL
 452 in TATTOO’s dual-stage training paradigm, we compare against a variant TATTOO (SFT only),
 453 which is trained solely on the first SFT stage. As shown in Table 3, under the Best-of- N evaluation,
 454 the second-stage RL policy optimization consistently improves performance over the SFT-only
 455 initialization. Specifically, we observe that the average accuracy across all three tasks improves from
 456 72.3% (SFT only) to 78.5% after RL training, yielding a total gain of 10.2%. This demonstrates that
 457 bootstrapping from SFT provides a solid initialization, while RL optimization further enhances our
 458 PRM’s reasoning and tool-use effectiveness during the verification process.

459 **Reward Shaping during RL Training.** Next, we analyze the effectiveness of each supervised component in
 460 our per-step reward signal s_i design (Eq. 3), with the
 461 ablation results reported in Table 3. Removing the tool-
 462 grounding term yields the largest drop (e.g., $\downarrow 4.0\%$ on
 463 TB-DA at $N=32$), highlighting its critical role in encour-
 464 aging effective tool use during RL training. In addition,
 465 excluding confidence calibration reduces performance by
 466 1.6% on average, showing its complementary effect in
 467 stabilizing reward signals. We also compare TATTOO
 468 with the original rule-based group-relative reward from
 469 GRPO, which yields only marginal improvement over
 470 SFT. Finally, Figure 6 visualizes the training dynamics of
 471 TATTOO and other variants during RL optimization.

472 **Additional Experiments.** Additional experiments, including ablations on the training coefficients
 473 and case studies on TATTOO’s effective tool usage, are provided in Appendix G.

475 6 RELATED WORKS

476 Reasoning over tables poses a unique challenge for LLMs, requiring them to bridge natural language
 477 understanding with structured reasoning over rows, columns, and cell values (Jin et al., 2022;
 478 Zhang et al., 2025a). Recent works (Tang et al., 2020; Iida et al., 2021; Deng et al., 2022) have
 479 investigated tabular reasoning on several downstream tasks, including table QA (Pasupat and Liang,
 480 2015b; Chen et al., 2020), table fact verification (Chen et al., 2019; Parikh et al., 2020), text-to-
 481 SQL (Mohammadjafari et al., 2024), etc. Early-stage tabular reasoning methods, such as TAPAS
 482 (Herzig et al., 2020) and TaBERT (Yin et al., 2020), encode table data into transformer-based encoder
 483 representations. Later methods leverage the capabilities of LLMs to apply either prompt engineering
 484 (Sui et al., 2023; Wang et al., 2024c) or supervised fine-tuning techniques (Su et al., 2024; Zhang
 485 et al., 2023) for enhanced tabular reasoning. More recent works, including the Table-R1 series (Wu
 et al., 2025b; Yang et al., 2025b; Jin et al., 2025) and Reasoning-Table (Lei et al., 2025), leverage RL



486 Figure 6: Training dynamics of TATTOO
 487 and ablated variants. We report the training
 488 reward across 280 training steps.

486 to acquire higher-quality reasoning paths during reasoning over tables. We leave additional related
 487 works on Process Reward Models and Tool Integration with RL in Appendix B.
 488

489 7 CONCLUSION

490 We introduced TaTToo, a novel tool-augmented thinking PRM tailored for tabular reasoning. By
 491 diagnosing why existing verifiers fail on table retrieval and schema interaction, we built a scalable
 492 pipeline with expert rationales, table prefixes, and tool-augmented verification, and trained our model
 493 via SFT followed by RL with reward shaping. TaTToo achieves comparable performance across
 494 five table benchmarks, surpassing strong PRMs with up to 9 \times parameter efficiency and generalizing
 495 across multiple TTS strategies. Our results underscore the importance of table-grounded reward
 496 supervision and point toward future directions in reward modeling for structured reasoning tasks.
 497

498 ETHICS STATEMENT

500 This work does not involve human subjects, sensitive personal information, or proprietary datasets.
 501 All datasets used in our experiments are publicly available table reasoning benchmarks, such as
 502 TabFact, FeTaQA, and WikiTableQuestions. We provide detailed descriptions of data processing
 503 steps in Section 5 and the Appendix D. The goal of our method is to improve process reward
 504 modeling for table reasoning, which we believe contributes positively to advancing trustworthy
 505 and interpretable reasoning with structured data. Nevertheless, we acknowledge that stronger table
 506 reasoning capabilities could be misused for generating misleading or biased tabular summaries if
 507 applied irresponsibly.

508 A potential limitation is that automated verification may propagate errors if tools or training labels
 509 are noisy. To mitigate this, our data curation pipeline integrates a retry-and-recovery procedure
 510 for all tool executions, and we filtered out cases where the tool outputs remained unstable after
 511 multiple attempts. Moreover, we explicitly evaluated TaTToo’s robustness under controlled tool-error
 512 conditions: across tasks, tool-error rates were low (1.9–5.8%), and TaTToo correctly assigned reward
 513 labels in 74–89% of error cases, demonstrating resilience to noisy or failed tool calls. Nonetheless,
 514 improving automated auditing mechanisms remains an important direction. Potential extensions
 515 include adaptive retry strategies, tool-aware correction of erroneous reasoning steps, and cross-tool
 516 consistency checks to detect unreliable tool outputs. While these directions are promising, the current
 517 version of TaTToo already incorporates concrete safeguards and empirical validation to ensure stable
 518 behavior in the presence of mild tool noise.

519 We encourage responsible use and adherence to the ICLR Code of Ethics.
 520

521 REPRODUCIBILITY STATEMENT

523 We have made careful efforts to ensure reproducibility. The main text describes our model architecture,
 524 training procedure, and evaluation protocols in detail (Sections 4–5). Additional hyperparameters,
 525 implementation details, and ablation study configurations are included in the Appendix F. All
 526 datasets are publicly available, and preprocessing steps are documented in Section 5. Theoretical
 527 analyses, including formal definitions of preference-based reward modeling and proofs of consistency
 528 guarantees, are provided in Appendix E. To further facilitate replication, we release our source code
 529 through an anonymized link https://anonymous.4open.science/r/iclr_TaTToo_code-C13F. Together, these resources ensure that our results can be independently verified.
 530

532 REFERENCES

534 Sandhini Agarwal, Lama Ahmad, Jason Ai, Sam Altman, Andy Applebaum, Edwin Arbus, Rahul K
 535 Arora, Yu Bai, Bowen Baker, Haiming Bao, et al. gpt-oss-120b & gpt-oss-20b model card. *arXiv*
 536 preprint *arXiv:2508.10925*, 2025.

537 Mubashara Akhtar, Abhilash Shankarampeta, Vivek Gupta, Arpit Patil, Oana Cocarascu, and Elena
 538 Simperl. Exploring the numerical reasoning capabilities of language models: A comprehensive
 539 analysis on tabular data. *arXiv preprint arXiv:2311.02216*, 2023.

540 Anthropic. Claude opus 4 and claude sonnet 4 system card. Technical report, Anthropic, 2025.
 541

542 Edward Beeching, Lewis Tunstall, and Sasha Rush. Scaling test-time compute with
 543 open models, 2024. URL <https://huggingface.co/spaces/HuggingFaceH4/blogpost-scaling-test-time-compute>.
 544

545 Bradley Brown, Jordan Juravsky, Ryan Ehrlich, Ronald Clark, Quoc V. Le, Christopher Ré, and
 546 Azalia Mirhoseini. Large language monkeys: Scaling inference compute with repeated sampling,
 547 2024. URL <https://arxiv.org/abs/2407.21787>.
 548

549 Wenhui Chen, Hongmin Wang, Jianshu Chen, Yunkai Zhang, Hong Wang, Shiyang Li, Xiyou Zhou,
 550 and William Yang Wang. Tabfact: A large-scale dataset for table-based fact verification. *arXiv
 551 preprint arXiv:1909.02164*, 2019.

552 Wenhui Chen, Hanwen Zha, Zhiyu Chen, Wenhan Xiong, Hong Wang, and William Wang. Hy-
 553 bridqa: A dataset of multi-hop question answering over tabular and textual data. *arXiv preprint
 554 arXiv:2004.07347*, 2020.

555 Xiusi Chen, Gaotang Li, Ziqi Wang, Bowen Jin, Cheng Qian, Yu Wang, Hongru Wang, Yu Zhang,
 556 Denghui Zhang, Tong Zhang, Hanghang Tong, and Heng Ji. Rm-r1: Reward modeling as reasoning,
 557 2025. URL <https://arxiv.org/abs/2505.02387>.
 558

559 Karl Cobbe, Vineet Kosaraju, Mohammad Bavarian, Mark Chen, Heewoo Jun, Lukasz Kaiser,
 560 Matthias Plappert, Jerry Tworek, Jacob Hilton, Reiichiro Nakano, et al. Training verifiers to solve
 561 math word problems. *arXiv preprint arXiv:2110.14168*, 2021.

562 Ganqu Cui, Lifan Yuan, Zefan Wang, Hanbin Wang, Wendi Li, Bingxiang He, Yuchen Fan, Tianyu
 563 Yu, Qixin Xu, Weize Chen, et al. Process reinforcement through implicit rewards. *arXiv preprint
 564 arXiv:2502.01456*, 2025.

565 Xiang Deng, Huan Sun, Alyssa Lees, You Wu, and Cong Yu. Turl: Table understanding through
 566 representation learning. *ACM SIGMOD Record*, 51(1):33–40, 2022.
 567

568 Yihe Dong, Jean-Baptiste Cordonnier, and Andreas Loukas. Attention is not all you need: Pure
 569 attention loses rank doubly exponentially with depth. In *International conference on machine
 570 learning*, pages 2793–2803. PMLR, 2021.

571 Jiazhao Feng, Shijue Huang, Xingwei Qu, Ge Zhang, Yujia Qin, Baoquan Zhong, Chengquan Jiang,
 572 Jinxin Chi, and Wanjun Zhong. Retool: Reinforcement learning for strategic tool use in llms.
 573 *arXiv preprint arXiv:2504.11536*, 2025a.
 574

575 Zhangying Feng, Qianglong Chen, Ning Lu, Yongqian Li, Siqi Cheng, Shuangmu Peng, Duyu Tang,
 576 Shengcai Liu, and Zhirui Zhang. Is prm necessary? problem-solving rl implicitly induces prm
 577 capability in llms. *arXiv preprint arXiv:2505.11227*, 2025b.

578 Xinyu Guan, Li Lyra Zhang, Yifei Liu, Ning Shang, Youran Sun, Yi Zhu, Fan Yang, and Mao Yang.
 579 rstar-math: Small llms can master math reasoning with self-evolved deep thinking. *arXiv preprint
 580 arXiv:2501.04519*, 2025.

581 Daya Guo, Dejian Yang, Haowei Zhang, Junxiao Song, Ruoyu Zhang, Runxin Xu, Qihao Zhu,
 582 Shirong Ma, Peiyi Wang, Xiao Bi, et al. Deepseek-r1: Incentivizing reasoning capability in llms
 583 via reinforcement learning. *arXiv preprint arXiv:2501.12948*, 2025.
 584

585 Jujie He, Tianwen Wei, Rui Yan, Jiacai Liu, Chaojie Wang, Yimeng Gan, Shiwen Tu, Chris Yuhao Liu,
 586 Liang Zeng, Xiaokun Wang, Boyang Wang, Yongcong Li, Fuxiang Zhang, Jiacheng Xu, Bo An,
 587 Yang Liu, and Yahui Zhou. Skywork-ol open series. <https://huggingface.co/Skywork>,
 588 November 2024a. URL <https://huggingface.co/Skywork>.
 589

590 Xinyi He, Jiaru Zou, Yun Lin, Mengyu Zhou, Shi Han, Zejian Yuan, and Dongmei Zhang. CoCoST:
 591 Automatic complex code generation with online searching and correctness testing. In Yaser
 592 Al-Onaizan, Mohit Bansal, and Yun-Nung Chen, editors, *Proceedings of the 2024 Conference on
 593 Empirical Methods in Natural Language Processing*, pages 19433–19451, Miami, Florida, USA,
 594 November 2024b. Association for Computational Linguistics. doi: 10.18653/v1/2024.emnlp-main.
 595 1082. URL <https://aclanthology.org/2024.emnlp-main.1082/>.
 596

594 Jonathan Herzig, Paweł Krzysztof Nowak, Thomas Müller, Francesco Piccinno, and Julian Mar-
 595 tin Eisenschlos. Tapas: Weakly supervised table parsing via pre-training. *arXiv preprint*
 596 *arXiv:2004.02349*, 2020.

597 Arian Hosseini, Xingdi Yuan, Nikolay Malkin, Aaron Courville, Alessandro Sordoni, and Rishabh
 598 Agarwal. V-star: Training verifiers for self-taught reasoners. *arXiv preprint arXiv:2402.06457*,
 599 2024.

600 Hiroshi Iida, Dung Thai, Varun Manjunatha, and Mohit Iyyer. Tabbie: Pretrained representations of
 601 tabular data. *arXiv preprint arXiv:2105.02584*, 2021.

602 Aaron Jaech, Adam Kalai, Adam Lerer, Adam Richardson, Ahmed El-Kishky, Aiden Low, Alec
 603 Helyar, Aleksander Madry, Alex Beutel, Alex Carney, et al. Openai o1 system card. *arXiv preprint*
 604 *arXiv:2412.16720*, 2024.

605 Nengzheng Jin, Joanna Siebert, Dongfang Li, and Qingcai Chen. A survey on table question
 606 answering: recent advances. In *China Conference on Knowledge Graph and Semantic Computing*,
 607 pages 174–186. Springer, 2022.

608 Rihui Jin, Zheyu Xin, Xing Xie, Zuoyi Li, Guilin Qi, Yongrui Chen, Xinbang Dai, Tongtong Wu,
 609 and Gholamreza Haffari. Table-r1: Self-supervised and reinforcement learning for program-based
 610 table reasoning in small language models. *arXiv preprint arXiv:2506.06137*, 2025.

611 Sham Kakade and John Langford. Approximately optimal approximate reinforcement learning. In
 612 *Proceedings of the nineteenth international conference on machine learning*, pages 267–274, 2002.

613 Muhammad Khalifa, Rishabh Agarwal, Lajanugen Logeswaran, Jaekyeom Kim, Hao Peng, Moontae
 614 Lee, Honglak Lee, and Lu Wang. Process reward models that think, 2025. URL <https://arxiv.org/abs/2504.16828>.

615 Fangyu Lei, Jinxiang Meng, Yiming Huang, Tinghong Chen, Yun Zhang, Shizhu He, Jun Zhao, and
 616 Kang Liu. Reasoning-table: Exploring reinforcement learning for table reasoning. *arXiv preprint*
 617 *arXiv:2506.01710*, 2025.

618 Peng Li, Yeye He, Dror Yashar, Weiwei Cui, Song Ge, Haidong Zhang, Danielle Rifinski Fainman,
 619 Dongmei Zhang, and Surajit Chaudhuri. Table-gpt: Table-tuned gpt for diverse table tasks. *arXiv*
 620 *preprint arXiv:2310.09263*, 2023a.

621 Wendi Li and Yixuan Li. Process reward model with q-value rankings. *arXiv preprint*
 622 *arXiv:2410.11287*, 2024.

623 Yinghui Li, Zishan Xu, Shaoshen Chen, Haojing Huang, Yangning Li, Yong Jiang, Zhongli Li,
 624 Qingyu Zhou, Hai-Tao Zheng, and Ying Shen. Towards real-world writing assistance: A chinese
 625 character checking benchmark with faked and misspelled characters. *CoRR*, abs/2311.11268,
 626 2023b. doi: 10.48550/ARXIV.2311.11268. URL <https://doi.org/10.48550/arXiv.2311.11268>.

627 Yinghui Li, Qingyu Zhou, Yuanzhen Luo, Shirong Ma, Yangning Li, Hai-Tao Zheng, Xuming Hu,
 628 and Philip S. Yu. When llms meet cunning questions: A fallacy understanding benchmark for
 629 large language models. *CoRR*, abs/2402.11100, 2024. doi: 10.48550/ARXIV.2402.11100. URL
 630 <https://doi.org/10.48550/arXiv.2402.11100>.

631 Hunter Lightman, Vineet Kosaraju, Yura Burda, Harri Edwards, Bowen Baker, Teddy Lee, Jan
 632 Leike, John Schulman, Ilya Sutskever, and Karl Cobbe. Let's verify step by step. *arXiv preprint*
 633 *arXiv:2305.20050*, 2023.

634 Hunter Lightman, Vineet Kosaraju, Yuri Burda, Harrison Edwards, Bowen Baker, Teddy Lee, Jan
 635 Leike, John Schulman, Ilya Sutskever, and Karl Cobbe. Let's verify step by step. In *The Twelfth*
 636 *International Conference on Learning Representations*, 2024. URL <https://openreview.net/forum?id=v8L0pN6EOi>.

637 Runze Liu, Junqi Gao, Jian Zhao, Kaiyan Zhang, Xiu Li, Biqing Qi, Wanli Ouyang, and Bowen
 638 Zhou. Can 1b llm surpass 405b llm? rethinking compute-optimal test-time scaling. *arXiv preprint*
 639 *arXiv:2502.06703*, 2025.

648 Dakota Mahan, Duy Van Phung, Rafael Rafailov, Chase Blagden, Nathan Lile, Louis Castricato,
 649 Jan-Philipp Fränken, Chelsea Finn, and Alon Albalak. Generative reward models. *arXiv preprint*
 650 *arXiv:2410.12832*, 2024.

651 Maxwell-Jia. AIME 2024 dataset. https://huggingface.co/datasets/Maxwell-Jia/AIME_2024, 2024. Accessed: 2025-05-15.

654 Ali Mohammadjafari, Anthony S Maida, and Raju Gottumukkala. From natural language to sql:
 655 Review of llm-based text-to-sql systems. *arXiv preprint arXiv:2410.01066*, 2024.

656 Niklas Muennighoff, Zitong Yang, Weijia Shi, Xiang Lisa Li, Li Fei-Fei, Hannaneh Hajishirzi, Luke
 657 Zettlemoyer, Percy Liang, Emmanuel Candès, and Tatsunori Hashimoto. s1: Simple test-time
 658 scaling, 2025. URL <https://arxiv.org/abs/2501.19393>.

660 Ankur Parikh, Xuezhi Wang, Sebastian Gehrmann, Manaal Faruqui, Bhuwan Dhingra, Diyi Yang,
 661 and Dipanjan Das. Totto: A controlled table-to-text generation dataset. In *EMNLP 2020*, pages
 662 1173–1186, 2020.

663 Panupong Pasupat and Percy Liang. Compositional semantic parsing on semi-structured tables.
 664 In Chengqing Zong and Michael Strube, editors, *Proceedings of the 53rd Annual Meeting of*
 665 *the Association for Computational Linguistics and the 7th International Joint Conference on*
 666 *Natural Language Processing (Volume 1: Long Papers)*, pages 1470–1480, Beijing, China, July
 667 2015a. Association for Computational Linguistics. doi: 10.3115/v1/P15-1142. URL <https://aclanthology.org/P15-1142/>.

668 Panupong Pasupat and Percy Liang. Compositional semantic parsing on semi-structured tables. In
 669 *Proceedings of the 53rd Annual Meeting of the Association for Computational Linguistics and*
 670 *the 7th International Joint Conference on Natural Language Processing of the Asian Federation*
 671 *of Natural Language Processing, ACL 2015, July 26-31, 2015, Beijing, China, Volume 1: Long*
 672 *Papers*, 2015b.

673 Cheng Qian, Emre Can Acikgoz, Qi He, Hongru Wang, Xiusi Chen, Dilek Hakkani-Tür, Gokhan
 674 Tur, and Heng Ji. Toolrl: Reward is all tool learning needs, 2025. URL <https://arxiv.org/abs/2504.13958>.

675 David Rein, Betty Li Hou, Asa Cooper Stickland, Jackson Petty, Richard Yuanzhe Pang, Julien Dirani,
 676 Julian Michael, and Samuel R. Bowman. Gpqa: A graduate-level google-proof q&a benchmark,
 677 2023. URL <https://arxiv.org/abs/2311.12022>.

678 John Schulman, Filip Wolski, Prafulla Dhariwal, Alec Radford, and Oleg Klimov. Proximal policy
 679 optimization algorithms. *arXiv preprint arXiv:1707.06347*, 2017.

680 Kwangwook Seo, Donguk Kwon, and Dongha Lee. Mt-raig: Novel benchmark and evaluation
 681 framework for retrieval-augmented insight generation over multiple tables. *arXiv preprint*
 682 *arXiv:2502.11735*, 2025.

683 Amrit Setlur, Chirag Nagpal, Adam Fisch, Xinyang Geng, Jacob Eisenstein, Rishabh Agarwal,
 684 Alekh Agarwal, Jonathan Berant, and Aviral Kumar. Rewarding progress: Scaling automated
 685 process verifiers for llm reasoning. *arXiv preprint arXiv:2410.08146*, 2024.

686 Zhihong Shao, Peiyi Wang, Qihao Zhu, Runxin Xu, Junxiao Song, Xiao Bi, Haowei Zhang,
 687 Mingchuan Zhang, YK Li, Y Wu, et al. Deepseekmath: Pushing the limits of mathematical
 688 reasoning in open language models, 2024. URL <https://arxiv.org/abs/2402.03300>, 2024.

689 Guangming Sheng, Chi Zhang, Zilingfeng Ye, Xibin Wu, Wang Zhang, Ru Zhang, Yanghua Peng,
 690 Haibin Lin, and Chuan Wu. Hybridflow: A flexible and efficient rlhf framework. *arXiv preprint*
 691 *arXiv: 2409.19256*, 2024.

692 Charlie Snell, Jaehoon Lee, Kelvin Xu, and Aviral Kumar. Scaling llm test-time compute optimally
 693 can be more effective than scaling model parameters. *arXiv preprint arXiv:2408.03314*, 2024.

694 Aofeng Su, Aowen Wang, Chao Ye, Chen Zhou, Ga Zhang, Guangcheng Zhu, Haobo Wang, Haokai
 695 Xu, Hao Chen, Haoze Li, et al. Tablegpt2: A large multimodal model with tabular data integration.
 696 *arXiv preprint arXiv:2411.02059*, 2024.

702 Yuan Sui, Jiaru Zou, Mengyu Zhou, Xinyi He, Lun Du, Shi Han, and Dongmei Zhang. Tap4ilm:
 703 Table provider on sampling, augmenting, and packing semi-structured data for large language
 704 model reasoning. *arXiv preprint arXiv:2312.09039*, 2023.

705 Yuan Sui, Mengyu Zhou, Mingjie Zhou, Shi Han, and Dongmei Zhang. Table meets llm: Can
 706 large language models understand structured table data? a benchmark and empirical study. In
 707 *Proceedings of the 17th ACM International Conference on Web Search and Data Mining*, pages
 708 645–654, 2024.

709 Nan Tang, Ju Fan, Fangyi Li, Jianhong Tu, Xiaoyong Du, Guoliang Li, Sam Madden, and Mourad
 710 Ouzzani. Rpt: relational pre-trained transformer is almost all you need towards democratizing data
 711 preparation. *arXiv preprint arXiv:2012.02469*, 2020.

712 Jonathan Uesato, Nate Kushman, Ramana Kumar, Francis Song, Noah Siegel, Lisa Wang, Antonia
 713 Creswell, Geoffrey Irving, and Irina Higgins. Solving math word problems with process- and
 714 outcome-based feedback, 2022. URL <https://arxiv.org/abs/2211.14275>.

715 Svitlana Vakulenko and Vadim Savenkov. Tableqa: Question answering on tabular data. *arXiv
 716 preprint arXiv:1705.06504*, 2017.

717 Jun Wang, Meng Fang, Ziyu Wan, Muning Wen, Jiachen Zhu, Anjie Liu, Ziqin Gong, Yan Song, Lei
 718 Chen, Lionel M Ni, et al. Openr: An open source framework for advanced reasoning with large
 719 language models. *arXiv preprint arXiv:2410.09671*, 2024a.

720 Peiyi Wang, Lei Li, Zhihong Shao, R. X. Xu, Damai Dai, Yifei Li, Deli Chen, Y. Wu, and Zhifang
 721 Sui. Math-shepherd: Verify and reinforce llms step-by-step without human annotations, 2024b.
 722 URL <https://arxiv.org/abs/2312.08935>.

723 Zilong Wang, Hao Zhang, Chun-Liang Li, Julian Martin Eisenschlos, Vincent Perot, Zifeng Wang,
 724 Lesly Miculicich, Yasuhisa Fujii, Jingbo Shang, Chen-Yu Lee, et al. Chain-of-table: Evolving
 725 tables in the reasoning chain for table understanding. *arXiv preprint arXiv:2401.04398*, 2024c.

726 Jian Wu, Linyi Yang, Dongyuan Li, Yuliang Ji, Manabu Okumura, and Yue Zhang. Mmqa: Evaluating
 727 llms with multi-table multi-hop complex questions. In *The Thirteenth International Conference on
 728 Learning Representations*, 2025a.

729 Xianjie Wu, Jian Yang, Linzheng Chai, Ge Zhang, Jiaheng Liu, Xinrun Du, Di Liang, Daixin Shu,
 730 Xianfu Cheng, Tianzhen Sun, et al. Tablebench: A comprehensive and complex benchmark for
 731 table question answering. *arXiv preprint arXiv:2408.09174*, 2024.

732 Zhenhe Wu, Jian Yang, Jiaheng Liu, Xianjie Wu, Changzai Pan, Jie Zhang, Yu Zhao, Shuangyong
 733 Song, Yongxiang Li, and Zhoujun Li. Table-r1: Region-based reinforcement learning for table
 734 understanding. *arXiv preprint arXiv:2505.12415*, 2025b.

735 An Yang, Beichen Zhang, Binyuan Hui, Bofei Gao, Bowen Yu, Chengpeng Li, Dayiheng Liu, Jian-
 736 hong Tu, Jingren Zhou, Junyang Lin, et al. Qwen2.5-math technical report: Toward mathematical
 737 expert model via self-improvement. *arXiv preprint arXiv:2409.12122*, 2024.

738 An Yang, Anfeng Li, Baosong Yang, Beichen Zhang, Binyuan Hui, Bo Zheng, Bowen Yu, Chang
 739 Gao, Chengen Huang, Chenxu Lv, et al. Qwen3 technical report, 2025a. URL <https://arxiv.org/abs/2505.09388>.

740 Jian Yang, Shuming Ma, Dongdong Zhang, Zhoujun Li, and Ming Zhou. Improving neural machine
 741 translation with soft template prediction. In Dan Jurafsky, Joyce Chai, Natalie Schluter, and Joel R.
 742 Tetreault, editors, *Proceedings of the 58th Annual Meeting of the Association for Computational
 743 Linguistics, ACL 2020, Online, July 5-10, 2020*, pages 5979–5989. Association for Computational
 744 Linguistics, 2020. doi: 10.18653/V1/2020.ACL-MAIN.531. URL <https://doi.org/10.18653/v1/2020.acl-main.531>.

745 Zheyuan Yang, Lyuhao Chen, Arman Cohan, and Yilun Zhao. Table-r1: Inference-time scaling for
 746 table reasoning, 2025b. URL <https://arxiv.org/abs/2505.23621>.

747 Yixin Ye, Zhen Huang, Yang Xiao, Ethan Chern, Shijie Xia, and Pengfei Liu. Limo: Less is more for
 748 reasoning. *arXiv preprint arXiv:2502.03387*, 2025.

756 Pengcheng Yin, Graham Neubig, Wen-tau Yih, and Sebastian Riedel. Tabert: Pretraining for joint
 757 understanding of textual and tabular data. *arXiv preprint arXiv:2005.08314*, 2020.

758

759 Tao Yu, Rui Zhang, Kai Yang, Michihiro Yasunaga, Dongxu Wang, Zifan Li, James Ma, Irene Li,
 760 Qingning Yao, Shanelle Roman, et al. Spider: A large-scale human-labeled dataset for complex
 761 and cross-domain semantic parsing and text-to-sql task. In *EMNLP 2018*, pages 3911–3921, 2018.

762 Dan Zhang, Sining Zhoubian, Ziniu Hu, Yisong Yue, Yuxiao Dong, and Jie Tang. Rest-mcts*: Llm
 763 self-training via process reward guided tree search. *arXiv preprint arXiv:2406.03816*, 2024.

764

765 Tianshu Zhang, Xiang Yue, Yifei Li, and Huan Sun. Tablellama: Towards open large generalist
 766 models for tables. *arXiv preprint arXiv:2311.09206*, 2023.

767

768 Xuanliang Zhang, Dingzirui Wang, Longxu Dou, Qingfu Zhu, and Wanxiang Che. A survey of table
 769 reasoning with large language models. *Frontiers of Computer Science*, 19(9):199348, 2025a.

770

771 Zhenru Zhang, Chujie Zheng, Yangzhen Wu, Beichen Zhang, Runji Lin, Bowen Yu, Dayiheng Liu,
 772 Jingren Zhou, and Junyang Lin. The lessons of developing process reward models in mathematical
 773 reasoning. *arXiv preprint arXiv:2501.07301*, 2025b.

774

775 Jian Zhao, Runze Liu, Kaiyan Zhang, Zhimu Zhou, Junqi Gao, Dong Li, Jiafei Lyu, Zhouyi Qian,
 776 Biqing Qi, Xiu Li, and Bowen Zhou. Genprm: Scaling test-time compute of process reward models
 777 via generative reasoning, 2025. URL <https://arxiv.org/abs/2504.00891>.

778

779 Lianmin Zheng, Wei-Lin Chiang, Ying Sheng, Siyuan Zhuang, Zhanghao Wu, Yonghao Zhuang,
 780 Zi Lin, Zhuohan Li, Dacheng Li, Eric Xing, et al. Judging llm-as-a-judge with mt-bench and
 781 chatbot arena. *Advances in Neural Information Processing Systems*, 36:46595–46623, 2023.

782

783 Yaowei Zheng, Richong Zhang, Junhao Zhang, Yanhan Ye, Zheyuan Luo, Zhangchi Feng, and
 784 Yongqiang Ma. Llamafactory: Unified efficient fine-tuning of 100+ language models. In *Proceedings of the 62nd Annual Meeting of the Association for Computational Linguistics (Volume 3: System Demonstrations)*, Bangkok, Thailand, 2024. Association for Computational Linguistics.
 785 URL <http://arxiv.org/abs/2403.13372>.

786

787 Jialun Zhong, Wei Shen, Yanzeng Li, Songyang Gao, Hua Lu, Yicheng Chen, Yang Zhang, Wei
 788 Zhou, Jinjie Gu, and Lei Zou. A comprehensive survey of reward models: Taxonomy, applications,
 789 challenges, and future. *arXiv preprint arXiv:2504.12328*, 2025.

790

791 Victor Zhong, Caiming Xiong, and Richard Socher. Seq2sql: Generating structured queries from
 792 natural language using reinforcement learning. *CoRR*, 2017.

793

794 Jiaru Zou, Ling Yang, Jingwen Gu, Jiahao Qiu, Ke Shen, Jingrui He, and Mengdi Wang. Reasonflux-
 795 prm: Trajectory-aware prms for long chain-of-thought reasoning in llms. *arXiv preprint
 796 arXiv:2506.18896*, 2025.

797

798

799

800

801

802

803

804

805

806

807

808

809

810 TABLE OF CONTENTS
811

813	A The Use of LLMs	17
814		
815	B Additional Related Work	17
816		
817	C Detailed Error Analysis	18
818		
820	D TATTOO Data Curation Pipeline	19
821		
822	E Proof of Theorem 4.1	20
823		
824	F Experimental Setups	22
825		
826	F.1 Policy Model Configurations	22
827	F.2 Evaluation Dataset Details	22
828	F.3 Training Details	23
829		
830		
831	G Additoinal Experiments	23
832		
833	G.1 Ablation Study on TATTOO	23
834	G.2 Case Study on TATTOO	23
835	G.3 Performance Gain of TATTOO with Increasing Number of Responses	23
836		
837		
838	H Limitations and Broader Impacts	24
839		
840	I TATTOO on Stronger Policy Models	25
841		
842	J Comparison with ORM Baselines	26
843		
844	K Comparison with Raw Qwen3-8B as a Step-Level Verifier	27
845		
846	L Integrating TaTToo with RL-Trained Table-R1	27
847		
848		
849	M Effeciency Analyses on TATTOO	28
850		
851		
852		
853		
854		
855		
856		
857		
858		
859		
860		
861		
862		
863		

864
865
866
867

Appendix

868
869
870
871
872
873
874
875
876

A THE USE OF LLMs

877
878
879
880
881
882
883
884
885
886
887
888
889
890
891
892
893
894
895
896
897
898
899
900
901
902
903
904
905
906
907
908
909
910
911
912
913
914
915
916
917

LLMs were used in this work in two main capacities. First, they served as the *base models* whose outputs were ranked and evaluated by our proposed TablePRM framework. We tested across a variety of publicly available pre-trained models, including Qwen and LLaMA families, to ensure robustness and generality, as described in Section 5 and Appendix F. Second, during the construction of preference pairs for supervision, we used LLM-generated responses as candidates, which were then compared and ranked according to factual consistency with gold tables. In addition, LLMs were used in a limited capacity for writing assistance, specifically to improve phrasing and readability of the manuscript. They did not contribute to research design, methodological innovations, or experimental results; all scientific contributions are the responsibility of the authors.

900
901
902
903
904
905
906
907
908
909
910
911
912
913
914
915
916
917

B ADDITIONAL RELATED WORK

900
901
902
903
904
905
906
907
908
909
910
911
912
913
914
915
916
917

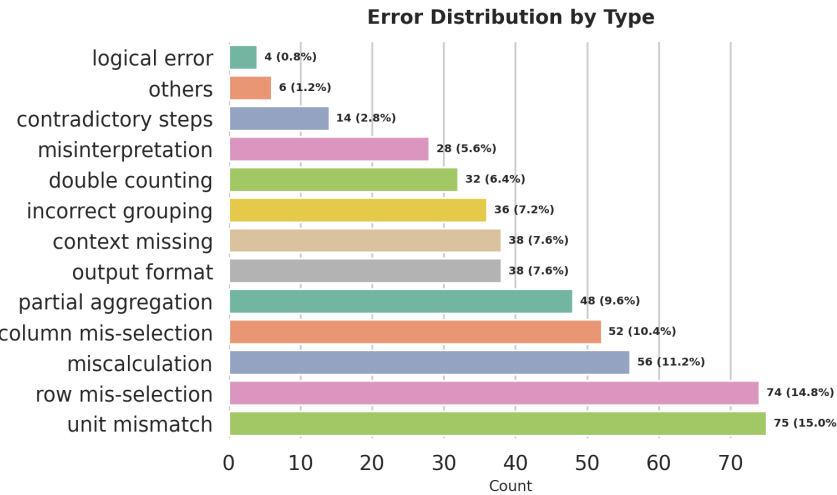
Table Question Answering. The evolution of Table Question Answering (Table QA) research (Jin et al., 2022) has been propelled by the creation of sophisticated evaluation resources that facilitate semantic parsing capabilities (Yang et al., 2020; Li et al., 2023b; 2024). Foundational works, including WTQ (Pasupat and Liang, 2015a) and TabFact (Chen et al., 2019), established initial evaluation paradigms through Wikipedia-derived HTML table QA pairs. Structured supervision has also been explored in alternative benchmarks such as WikiSQL (Zhong et al., 2017) and Spider (Yu et al., 2018), where logical expressions serve as explicit annotations to encourage systematic reasoning. More recent studies such as MultiTableQA (Wu et al., 2024), MT-RAIG (Seo et al., 2025), and MMQA (Wu et al., 2025a) has shifted towards multi-hop reasoning.

900
901
902
903
904
905
906
907
908
909
910
911
912
913
914
915
916
917

PRMs for Test-time Scaling. Process Reward Models (PRMs) (Lightman et al., 2024; Uesato et al., 2022; Zhang et al., 2024) deliver fine-grained, step-level feedback to guide model reasoning, assigning intermediate rewards to individual reasoning steps rather than only judging final answers (Guan et al., 2025; Chen et al., 2025). Prominent PRMs, including Math-Shepherd (Wang et al., 2024b), Skywork-PRM (He et al., 2024a), and the Qwen2.5-Math-PRM family (Zhang et al., 2025b), are trained using a mix of human annotations and synthesized supervision to score model-generated solution steps across domains such as math (Maxwell-Jia, 2024), scientific reasoning (Rein et al., 2023), and programming (He et al., 2024b); more recently, Think-PRM proposes a generative verifier to produce long-chain CoT evaluations (Khalifa et al., 2025). PRMs have been incorporated into training-time optimization as reward signals via step-verified online RL and verifier-guided self-training (Li and Li, 2024; Guan et al., 2025; Cui et al., 2025), and into inference-time scaling by coupling step-level scoring with search/decoding strategies (Zhao et al., 2025; Khalifa et al., 2025), including beam search, reward-guided tree search, and Best-of-N sampling.

900
901
902
903
904
905
906
907
908
909
910
911
912
913
914
915
916
917

Discriminative vs. Generative PRM. In general, PRMs can be categorized as discriminative and generative evaluators (Zhong et al., 2025). A **discriminative PRM** treats verification as classification, directly predicting the correctness of each reasoning step with a scalar score. It is typically trained on step-level labels using cross-entropy loss, making it heavily reliant on step-level reward annotations. A **generative PRM** instead frames verification as conditional generation. It is trained with the standard language modeling objective to first generate rationales and then verify each step’s correctness via a judgment token (e.g., [correct, incorrect]).

918 C DETAILED ERROR ANALYSIS
919
920937 Figure 7: Error distribution over 500 incorrect LRM responses after Best-of-N. The errors are grouped
938 into 13 predefined types, with the majority arising from table retrieval and schema interaction.
939940 In Section 3, we perform a fine-grained error analysis on 500 erroneous responses sampled after
941 Best-of- N selection with Qwen2.5-Math-PRM-72B, to better understand the limitations of LRMs and
942 PRMs. Each response is inspected and categorized by human experts into 13 predefined error types,
943 covering both reasoning and table-specific mistakes. Figure 7 illustrates the overall error distribution.
944945 **Error Type Distribution.** The most frequent errors are *unit mismatch* (15.0%), *row mis-selection*
946 (14.8%), and *miscalculation* (11.2%). Other common issues include *column mis-selection* (10.4%),
947 *partial aggregation* (9.6%), and missing or incomplete *context* (7.6%). Less frequent but still notable
948 categories include *output format errors*, *incorrect grouping*, *double counting*, *misinterpretation*, and
949 *contradictory steps*. A small portion of errors is grouped under *others* and *logical errors*. This diverse
950 distribution highlights that model failures are not restricted to arithmetic slips but extend to schema
951 understanding and structural reasoning.
952953 **Mapping to Reasoning-Step Categories.** To reveal deeper patterns, we align the 13 error types
954 with four reasoning-step categories reflecting the typical flow of LRMs:
955

- **Table Retrieval Step:** Includes row/column mis-selection, unit mismatch, and partial aggregation. These account for 47.7% of total errors, indicating difficulty in locating and extracting the correct table region.
- **Schema Interaction Step:** Covers miscalculation, grouping mistakes, double counting, and misinterpretation of table semantics. This represents 34.3% of errors, reflecting challenges in reasoning over structured contents once retrieved.
- **Inner-Thinking Step:** Logical errors or contradictory reasoning steps independent of table contents. These contribute 12.0% of total errors, suggesting LRMs remain relatively competent in pure logical chains compared to table-centric operations.
- **Others:** Errors arising from context omission or improper output formatting.

956 **Key Findings.** The analysis confirms that most model weaknesses lie in table-related operations,
957 including table retrieval and schema interaction, rather than general logical reasoning. PRMs, when
958 supervising such steps, face greater challenges since they must not only validate the correctness of
959 reasoning but also verify alignment between the retrieved sub-table and the query.
960
961

972 **D TATTOO DATA CURATION PIPLINE**
973974 We design a large-scale data curation pipeline that simulates real-world scenarios of PRM tool use
975 and step verification at scale. As illustrated in Figure 4, there are three main stages:
976977 **Reasoning Trajectory Generation.** We begin by collecting trajectory responses from expert LRM
978 (e.g., DeepSeek-R1 (Guo et al., 2025) and Claude-Opus-4.1 (Anthropic, 2025)) on table-based
979 questions drawn from diverse benchmarks, including TableInstruct (Wu et al., 2024), HybridQA (Chen
980 et al., 2020), ToTTo (Parikh et al., 2020), and WikiTQ (Pasupat and Liang, 2015b).
981982 We generate multiple model responses per query, capturing both correct and incorrect reasoning
983 patterns. We then adopt a dual-verification procedure (Feng et al., 2025a), where both human
984 annotators and expert LLMs are employed to examine and filter out low-quality or incomplete CoT
985 data. Through this, we receive a high-quality set of LRM’s output responses $\mathcal{T}_{\text{pool}}$ for subsequent
986 data labeling.
987988 **Verification Synthesis & Reward Assignment.** Our next step is to provide step-level verification
989 rationales and assign PRM step-reward labels for each candidate response in $\mathcal{T}_{\text{pool}}$. To this end, we
990 first identify the table retrieval and schema interaction steps within each response in $\mathcal{T}_{\text{pool}}$:
991992 *Table retrieval steps* - We first extract the retrieved sub-table from each step. Then we apply LLM-as-
993 a-judge to evaluate whether retrieved contents are accurate and provide complete rationales for the
994 judgment. We assign step-level table reward $r_{i,\text{tab}} \in \{-1, 1\}$ (in Eq. 1) based on the correctness of
995 the retrieval, while setting $r_{i,\text{rea}}$ to 0. This reward supervision explicitly trains PRMs to recognize if
996 the retrieved sub-table aligns with the input query, addressing the limitation shown in *Takeaway 1*.
997998 *Schema interaction steps* - We collect the sub-table retrieved from the preceding table retrieval step
999 and use it as a table prefix. If the retrieval is incorrect, we manually replace it with the correct
1000 sub-table corresponding to the query. We then prepend this table prefix to the verification rationale
1001 generated by LLM-as-a-judge. Finally, we assign the PRM’s step-level table reward $r_{i,\text{tab}} \in \{-1, 1\}$
1002 based on the correctness of the schema interaction, and $r_{i,\text{rea}}$ to 0. By explicitly attaching the retrieved
1003 sub-table to each schema interaction step, we mitigate the dependencies issue noted in *Takeaway 2*.
10041005 *Other steps without table operations involved* - We directly query an expert LLM (DeepSeek-R1) to
1006 generate verification rationales. We assign the PRM’s step-level reasoning reward $r_{i,\text{rea}} \in \{-1, 1\}$
1007 based on the correctness of the reasoning, while setting the table reward $r_{i,\text{tab}}$ to 0.
10081009 **Tool Use Synthesis.** To help PRMs learn to leverage tools for more accurate verification, we augment
1010 the collected verification rationales by incorporating tool invocation, execution, and feedback into
1011 the verification steps. Specifically, whenever the model’s inner reasoning involves a calculation or
1012 table lookup operation, we replace it with the corresponding tool call and its execution result. We
1013 primarily employ two types of tools:
10141015 *Computation tools* - Applying Python or SQL code snippets for arithmetic or aggregation operations.
1016 E.g., if a step verifies the sum of a table column, we replace the model’s manual calculation with a
1017 code snippet that executes the summation and returns the result.
10181019 *Table lookup tools* - Locating and extracting specific rows, columns, or cells from the table. E.g.,
1020 if a step requires referencing a sub-table cell value during the verification, we replace the model’s
1021 self-extraction with an explicit lookup tool call that retrieves the corresponding entry.
10221023 By integrating verification processes with code snippets and real-time interpreter feedback, we
1024 construct roughly 60k data for TATTOO’s verification reasoning and tool usage.
1025

1026 **E PROOF OF THEOREM 4.1**
 1027

1028 **Notational conventions.** We use \mathbf{s}_i for a state, a_i for an action, π for the current policy, and π' for
 1029 the updated policy. The advantage is defined as
 1030

$$1031 A^\pi(\mathbf{s}_i, a_i) = Q^\pi(\mathbf{s}_i, a_i) - V^\pi(\mathbf{s}_i). \quad (6)$$

1032 The PRM signal at a step is the overall process reward, defined in Eq.2. For a fixed \mathbf{s}_i , we
 1033 write $\mathbb{E}_\pi[\cdot] \equiv \mathbb{E}_{a_i \sim \pi(\cdot | \mathbf{s}_i)}[\cdot]$, $\text{Var}_\pi[\cdot] \equiv \text{Var}_{a_i \sim \pi(\cdot | \mathbf{s}_i)}[\cdot]$, and $\text{Cov}_\pi(r_{i,\text{rea}}(\mathbf{s}_i, a_i), r_{i,\text{rea}}(\mathbf{s}_i, a_i)) \equiv$
 1034 $\text{Cov}_{a_i \sim \pi(\cdot | \mathbf{s}_i)}(r_{i,\text{rea}}(\mathbf{s}_i, a_i), r_{i,\text{rea}}(\mathbf{s}_i, a_i))$. Expectations over states use the subscript explicitly, e.g.,
 1035 $\mathbb{E}_{\mathbf{s}_i \sim \rho}[\cdot]$. We use $d_\rho^{\pi'}$ for the state distribution induced by the policy π' starting from the initial
 1036 distribution ρ . Finally, $X \gtrsim Y$ means there exists a universal constant $c > 0$, independent of
 1037 $(\pi, \pi', \mathbf{s}_i)$, such that $X \geq cY$.
 1038

1039 We start the proof by introducing two standard lemmas that will be used repeatedly; both are
 1040 well-known results in the RL literature, and we omit their proofs here for brevity.
 1041

1042 **Lemma E.1 (Performance Difference Lemma (PDL)).** *For any pair of policies π and π' defined
 1043 over the same Markov decision process with initial state distribution ρ , the following identity holds:*

$$1043 \mathbb{E}_{\mathbf{s}_i \sim \rho} \left[V^{\pi'}(\mathbf{s}_i) - V^\pi(\mathbf{s}_i) \right] = \mathbb{E}_{\mathbf{s}_i \sim d_\rho^{\pi'}} \mathbb{E}_{a_i \sim \pi'(\cdot | \mathbf{s}_i)} [A^\pi(\mathbf{s}_i, a_i)].$$

1044 See proof of Lemma 6.1 in (Kakade and Langford, 2002).
 1045

1046 **Lemma E.2 (Natural policy gradient (NPG) update form).** *Fix a step size $\gamma > 0$. If the NPG
 1047 update is guided by the signal $A^\pi(\mathbf{s}_i, a_i) + r_i(\mathbf{s}_i, a_i)$, then*

$$1047 \begin{aligned} \pi'(a_i | \mathbf{s}_i) &\propto \pi(a_i | \mathbf{s}_i) \exp\left(\gamma(A^\pi(\mathbf{s}_i, a_i) + r_i(\mathbf{s}_i, a_i))\right), \\ 1048 Z^\pi(\mathbf{s}_i) &\triangleq \sum_{a_i} \pi(a_i | \mathbf{s}_i) \left[\exp\left(\gamma(A^\pi(\mathbf{s}_i, a_i) + r_i(\mathbf{s}_i, a_i))\right) \right], \\ 1049 \text{so that } \frac{\pi'(a_i | \mathbf{s}_i)}{\pi(a_i | \mathbf{s}_i)} &= \frac{\exp\left(\gamma(A^\pi(\mathbf{s}_i, a_i) + r_i(\mathbf{s}_i, a_i))\right)}{Z^\pi(\mathbf{s}_i)}. \end{aligned} \quad (7)$$

1050 See proof of Lemma F.2 in (Setlur et al., 2024). Next, we restate Theorem 4.1 in the following
 1051 proposition.
 1052

1053 **Proposition E.3 (Full-strength policy improvement lower bound).** *Let π' be the NPG update in
 1054 Lemma E.2. We can have:*

$$1054 \begin{aligned} \mathbb{E}_{\mathbf{s}_i \sim \rho} \left[V^{\pi'}(\mathbf{s}_i) - V^\pi(\mathbf{s}_i) \right] &\gtrsim \mathbb{E}_{\mathbf{s}_i \sim \rho} \left[\underbrace{\text{Var}_\pi[r_{i,\text{rea}}(\mathbf{s}_i, a_i)]}_{\text{distinguishability (reasoning reward)}} + \underbrace{\text{Var}_\pi[r_{i,\text{tab}}(\mathbf{s}_i, a_i)]}_{\text{distinguishability (table reward)}} \right. \\ 1055 &\quad \left. + 2 \underbrace{\text{Cov}_\pi(r_{i,\text{rea}}(\mathbf{s}_i, a_i), r_{i,\text{tab}}(\mathbf{s}_i, a_i))}_{\text{alignment between } r_{i,\text{rea}} \text{ and } r_{i,\text{tab}}} + \underbrace{\mathbb{E}_\pi[r_{i,\text{tab}}(\mathbf{s}_i, a_i) A^\pi(\mathbf{s}_i, a_i)]}_{\text{alignment of } r_{i,\text{tab}} \text{ with } A^\pi} + \underbrace{\mathbb{E}_\pi[r_{i,\text{rea}}(\mathbf{s}_i, a_i) A^\pi(\mathbf{s}_i, a_i)]}_{\text{alignment of } r_{i,\text{rea}} \text{ with } A^\pi} \right]. \end{aligned} \quad (8)$$

1056 *Proof of Proposition E.3.* We now combine the performance difference lemma with the NPG update
 1057 to derive a variance-alignment lower bound, while first retaining the covariance term between the
 1058 reward components. By Lemma E.1, we have
 1059

$$1060 \mathbb{E}_{\mathbf{s}_i \sim \rho} \left[V^{\pi'}(\mathbf{s}_i) - V^\pi(\mathbf{s}_i) \right] = \mathbb{E}_{\mathbf{s}_i \sim d_\rho^{\pi'}} \mathbb{E}_{a_i \sim \pi'(\cdot | \mathbf{s}_i)} [A^\pi(\mathbf{s}_i, a_i)]. \quad (9)$$

1061 **Exponential tilting and a log-partition bound.** Let us define the log-partition at state \mathbf{s}_i by
 1062

$$1063 \log Z^\pi(\mathbf{s}_i) = \log \mathbb{E}_{a_i \sim \pi(\cdot | \mathbf{s}_i)} \exp\left(\gamma(A^\pi(\mathbf{s}_i, a_i) + r_i(\mathbf{s}_i, a_i))\right).$$

1064 From Lemma E.2, we have
 1065

$$1066 A^\pi(\mathbf{s}_i, a_i) = \frac{1}{\gamma} \log \frac{\pi'(a_i | \mathbf{s}_i)}{\pi(a_i | \mathbf{s}_i)} - r_i(\mathbf{s}_i, a_i) + \frac{1}{\gamma} \log Z^\pi(\mathbf{s}_i).$$

1080 Averaging over $a_i \sim \pi'(\cdot | \mathbf{s}_i)$, using $\mathbb{E}_{\pi'}[\log \frac{\pi'}{\pi}] \geq 0$, Jensen's inequality on $\log Z^\pi(\mathbf{s}_i)$ and
 1081 $\mathbb{E}_\pi[A^\pi(\mathbf{s}_i, a_i)] = 0$ gives
 1082

$$\mathbb{E}_{a_i \sim \pi'(\cdot | \mathbf{s}_i)}[A^\pi(\mathbf{s}_i, a_i)] \geq -\mathbb{E}_{a_i \sim \pi'(\cdot | \mathbf{s}_i)}[r_i(\mathbf{s}_i, a_i)] + \mathbb{E}_{a_i \sim \pi(\cdot | \mathbf{s}_i)}[r_i(\mathbf{s}_i, a_i)]. \quad (10)$$

1083 Plugging this into equation 9 yields the basic inner-product lower bound
 1084

$$\mathbb{E}_{\mathbf{s}_i \sim \rho}[V^{\pi'}(\mathbf{s}_i) - V^\pi(\mathbf{s}_i)] \geq \mathbb{E}_{\mathbf{s}_i \sim d_\rho^{\pi'}} \langle \pi'(\cdot | \mathbf{s}_i) - \pi(\cdot | \mathbf{s}_i), r_i(\mathbf{s}_i, \cdot) \rangle. \quad (11)$$

1085 Using first-order expansion of the exponential tilt implies
 1086

$$\langle \pi'(\cdot | \mathbf{s}_i) - \pi(\cdot | \mathbf{s}_i), r_i(\mathbf{s}_i, \cdot) \rangle \gtrsim (\text{Var}_\pi[r_i(\mathbf{s}_i, a_i)] + \mathbb{E}_\pi[r_i(\mathbf{s}_i, a_i) A^\pi(\mathbf{s}_i, a_i)]), \quad (12)$$

1087 Combining equation 11 and equation 12, and weakening $d_\rho^{\pi'}$ to ρ (componentwise monotonicity)
 1088 gives
 1089

$$\mathbb{E}_{\mathbf{s}_i \sim \rho}[V^{\pi'}(\mathbf{s}_i) - V^\pi(\mathbf{s}_i)] \gtrsim \mathbb{E}_{\mathbf{s}_i \sim \rho}[\text{Var}_\pi[r_i(\mathbf{s}_i, a_i)] + \mathbb{E}_\pi[r_i(\mathbf{s}_i, a_i) A^\pi(\mathbf{s}_i, a_i)]]. \quad (13)$$

1090 **Variance decomposition with covariance.** Next, using $r_i = r_{i,\text{rea}} + r_{i,\text{tab}}$, we have
 1091

$$\text{Var}_\pi[r_i(\mathbf{s}_i, a_i)] = \text{Var}_\pi[r_{i,\text{rea}}(\mathbf{s}_i, a_i)] + \text{Var}_\pi[r_{i,\text{tab}}(\mathbf{s}_i, a_i)] + 2 \text{Cov}_\pi(r_{i,\text{rea}}(\mathbf{s}_i, a_i), r_{i,\text{tab}}(\mathbf{s}_i, a_i)). \quad (14)$$

1092 Substituting into equation 13 complete our proof of Proposition E.3 (equation 8). \square
 1093

1094 **Covariance elimination under our reward design.** By construction in our setup (see Section 4.2),
 1095 for each state-action pair (\mathbf{s}_i, a_i) , the two components of the PRM signal, i.e., table reward and
 1096 reasoning reward, are *mutually exclusive*. Formally, we have
 1097

$$r_{i,\text{tab}}(\mathbf{s}_i, a_i) \in \{-1, 0, 1\}, \quad r_{i,\text{rea}}(\mathbf{s}_i, a_i) \in \{-1, 0, 1\}, \quad \text{and} \quad r_{i,\text{tab}}(\mathbf{s}_i, a_i) r_{i,\text{rea}}(\mathbf{s}_i, a_i) = 0.$$

1098 Policy-gradient updates are invariant to adding any per-state baseline, so we may center each
 1099 component without loss, i.e.,
 1100

$$\tilde{r}_{i,\text{rea}}(\mathbf{s}_i, a_i) = r_{i,\text{rea}}(\mathbf{s}_i, a_i) - \mathbb{E}_\pi[r_{i,\text{rea}}(\mathbf{s}_i, a_i)], \quad \tilde{r}_{i,\text{tab}}(\mathbf{s}_i, a_i) = r_{i,\text{tab}}(\mathbf{s}_i, a_i) - \mathbb{E}_\pi[r_{i,\text{tab}}(\mathbf{s}_i, a_i)].$$

1101 Mutual exclusivity yields $\mathbb{E}_\pi[\tilde{r}_{i,\text{rea}}(\mathbf{s}_i, a_i) \tilde{r}_{i,\text{tab}}(\mathbf{s}_i, a_i)] = 0$, hence $\text{Cov}_\pi(\tilde{r}_{i,\text{rea}}, \tilde{r}_{i,\text{tab}}) = 0$ and
 1102

$$\text{Var}_\pi[\tilde{r}_i(\mathbf{s}_i, a_i)] = \text{Var}_\pi[\tilde{r}_{i,\text{rea}}(\mathbf{s}_i, a_i)] + \text{Var}_\pi[\tilde{r}_{i,\text{tab}}(\mathbf{s}_i, a_i)], \quad \tilde{r}_i \triangleq \tilde{r}_{i,\text{rea}} + \tilde{r}_{i,\text{tab}}.$$

1103 Plugging these centered quantities into the bounds of Proposition E.3 (which is NPG-invariant under
 1104 per-state centering) gives exactly Theorem 4.1's inequality:
 1105

$$\begin{aligned} \mathbb{E}_{\mathbf{s}_i \sim \rho}[V^{\pi'}(\mathbf{s}_i) - V^\pi(\mathbf{s}_i)] &\gtrsim \mathbb{E}_{\mathbf{s}_i \sim \rho}[\text{Var}_\pi[r_{i,\text{rea}}(\mathbf{s}_i, a_i)] + \text{Var}_\pi[r_{i,\text{tab}}(\mathbf{s}_i, a_i)] \\ &\quad + \mathbb{E}_\pi[r_{i,\text{tab}}(\mathbf{s}_i, a_i) A^\pi(\mathbf{s}_i, a_i)] + \mathbb{E}_\pi[r_{i,\text{rea}}(\mathbf{s}_i, a_i) A^\pi(\mathbf{s}_i, a_i)]], \end{aligned} \quad (15)$$

1106 which completes the proof of Theorem 4.1. \square
 1107

1108 **Remarks.** (i) Proposition E.3 is strictly more general; Theorem 4.1 follows as a corollary under
 1109 mutual exclusivity plus per-state centering (baseline invariance). (ii) Mutual exclusivity alone
 1110 yields $\mathbb{E}_\pi[r_{i,\text{rea}} r_{i,\text{tab}}] = 0$, but per-state centering is what ensures $\text{Cov}_\pi(r_{i,\text{rea}}, r_{i,\text{tab}}) = 0$. (iii) The
 1111 alignment term necessarily uses the composite signal r_i because the NPG step is guided by $A^\pi + r_i$.
 1112

1113
 1114
 1115
 1116
 1117
 1118
 1119
 1120
 1121
 1122
 1123
 1124
 1125
 1126
 1127
 1128
 1129
 1130
 1131
 1132
 1133

1134 F EXPERIMENTAL SETUPS
11351136 F.1 POLICY MODEL CONFIGURATIONS
1137

1138 In our experiments, we adopt an LRM DeepSeek-R1-Distill-Qwen-14B (Guo et al., 2025) as the
1139 downstream policy model. During inference, we configure the model with a temperature of 0.7, a
1140 maximum generation length of 16,384 tokens, and top- p sampling with $p = 0.95$. We evaluate the
1141 LRM on several inference-time scaling strategies:

1142 **Best-of-N (BoN).** The policy model generates N candidate responses independently. A verifier
1143 (PRM) scores each response, and the final output is selected based on a voting or scoring method.

1144 **Beam Search.** Given beam width N and branching factor M , the model generates N initial steps.
1145 The verifier then selects the top N/M continuations, and the model expands each with M new
1146 candidates. This process repeats until termination, enabling guided exploration of high-quality
1147 reasoning paths.

1148 **Diverse Verifier Tree Search (DVTS).** DVTS is a variant of beam search where the search process
1149 is divided into multiple subtrees. Each subtree is explored independently using verifier-guided
1150 expansions, with candidates selected at every step based on PRM scores.

1151 **Majority Voting.** After generating multiple responses, the final answer is determined by simple
1152 majority over identical outputs, regardless of intermediate step scores. This method provides a
1153 baseline aggregation mechanism.

1154 **LLM-as-a-Judge.** Instead of relying solely on PRMs, a separate LLM is prompted to compare and
1155 evaluate candidate responses directly, selecting the most plausible or logically consistent output.

1161 F.2 EVALUATION DATASET DETAILS
1162

1163 **TableBench (Wu et al., 2024).** TableBench is a comprehensive benchmark specifically designed to
1164 evaluate the reasoning abilities of LLMs over tabular data. It consists of 3,681 unique tables drawn
1165 from diverse domains such as finance, sports, politics, and science, with each table containing on
1166 average 16.7 rows and 6.7 columns. The dataset emphasizes numerical reasoning, with over 65%
1167 of table cells containing numerical values. TableBench questions are organized into four major
1168 categories: fact-checking, numerical reasoning, data analysis, further divided into 18 subcategories,
1169 yielding a total of 886 carefully annotated samples. Each question typically requires 6.3 reasoning
1170 steps, making the dataset significantly more complex than prior TableQA corpora.

1171 **WikiTableQuestions (WTQ) (Pasupat and Liang, 2015b).** The WikiTableQuestions dataset
1172 introduces question answering over semi-structured HTML tables, aiming to test both compositional
1173 reasoning and domain generalization. It comprises 22,033 natural language questions paired with
1174 2,108 Wikipedia tables, where the training and test tables are disjoint to ensure generalization to
1175 unseen schemas. The tables are semi-structured and heterogeneous, often containing multi-part
1176 cell values (e.g., “Beijing, China”) that require normalization into multiple semantic types such as
1177 numbers or dates. Questions range from simple lookups to highly compositional queries involving
1178 comparison, aggregation, arithmetic, and superlatives. Each table contains at least 8 rows and 5
1179 columns, and the question collection was conducted with quality control through multiple annotators.

1180 **MMQA (Wu et al., 2025a)** MMQA is a large-scale benchmark for evaluating LLMs on multi-table
1181 and multi-hop question answering. The benchmark includes a total of 3,312 relational tables across
1182 138 domains, where each instance consists of two or three interlinked tables. The dataset features
1183 5,000 multi-table samples, annotated with natural language questions, SQL queries, gold answers,
1184 and explicit primary/foreign key relations. To ensure annotation quality, foreign and primary keys
1185 were labeled by human experts with inter-annotator agreement exceeding 80%. MMQA questions
1186 span four main categories, including numerical, list, count, and select, with an average length of
1187 77–85 tokens, reflecting their compositional complexity.

1188
1189

F.3 TRAINING DETAILS

1190 We train TATTOO using the off-the-shelf Qwen-3-8B model (Yang et al., 2025a) on our curated
 1191 60k dataset. For supervised fine-tuning, we adopt the LLaMA-Factory framework (Zheng et al.,
 1192 2024). The training setup uses a learning rate of 1×10^{-5} , a weight decay of 1×10^{-4} , a maximum
 1193 sequence length of 20,000, and is run for 3 epochs. For the RL training stage, we adopt the VeRL
 1194 framework (Sheng et al., 2024) to further optimize the SFT checkpoint via policy optimization. The
 1195 model is trained with a batch size of 32, generating 8 samples per question as the group size, and is
 1196 run for 3 epochs. During inference, we use the OpenR framework (Wang et al., 2024a) to deploy
 1197 our trained TATTOO-8B, which serves as a verifier to guide the downstream LRM under different
 1198 test-time scaling strategies.
 1199

1200
1201
1202
1203

G ADDITIONAL EXPERIMENTS

G.1 ABLATION STUDY ON TATTOO

1204 Table 4: Ablation on confidence calibration λ_{cal} .
1205

N=32	TB-NR	TB-FC	TB-DA
0.3	76.8	80.9	33.1
0.5	77.3	81.3	33.6
0.8	78.1	82.0	34.3
1.0	78.5	81.4	33.8

1204 Table 5: Ablation on tool-grounding λ_{tool} .
1205

N=32	TB-NR	TB-FC	TB-DA
0.1	75.2	76.3	30.8
0.5	75.9	76.9	32.2
1.0	78.1	82.0	34.3
1.3	77.5	81.2	34.6

1213
1214
1215
1216
1217
1218
1219

Ablations on λ_{cal} and λ_{tool} . In Eq. 3, we use λ_{cal} and λ_{tool} as tunable coefficients to balance the contributions of the corresponding reward terms in GRPO. To examine their influence, we separately train our verifier model (initialized from the same SFT checkpoint) by varying $\lambda_{\text{cal}} \in \{0.3, 0.5, 0.8, 1.0\}$ and $\lambda_{\text{tool}} \in \{0.1, 0.5, 1.0, 1.5\}$ during RL, and then evaluate on TableBench with $N = 32$. As shown in Table 4 and 5, performance improves as λ_{cal} increases, peaking at 0.8–1.0. For λ_{tool} , accuracy rises steadily and is strongest around 1.0–1.3. These results empirically confirm the effectiveness of confidence calibration and tool-grounding in enhancing TTS.

1220
1221

G.2 CASE STUDY ON TATTOO

1222
1223
1224
1225
1226
1227
1228
1229
1230

As shown in Figure 9, we present a case study on TATTOO illustrating the difference between the verification processes at the two training stages on a specific instance in Figure 9 (Appendix G.2). When facing the same step (Step 3), the SFT-stage relies on inner text reasoning to verify the calculation, but introduces numerical errors that lead to incorrect justification of the step’s correctness. In contrast, the RL-stage learns to leverage the computation tool with concise Python code, ensuring accurate calculations and thereby providing more reliable reward supervision on the policy model’s responses. In addition, we randomly sample 500 trajectories from both stages of TATTOO on the same set of inputs and observe a 26.3% improvement in the tool-integration ratio after RL training, indicating our model learns to utilize tools better for step-level verification during RL rollouts.

1231
1232
1233
1234
1235
1236
1237
1238
1239
1240
1241

G.3 PERFORMANCE GAIN OF TATTOO WITH INCREASING NUMBER OF RESPONSES

Figure 8 presents the best-of- N performance on TB-NR. We observe that baseline PRMs such as Qwen2.5-Math-PRM-72B and GenPRM-32B quickly saturate beyond $N=16$, achieving only marginal improvements at larger N . Skywork-PRM-7B shows even weaker scalability, plateauing below 71%. In contrast, TATTOO continues to improve steadily as N increases, reaching 78.3% at $N=32$, the highest among all models despite having significantly fewer parameters (8B). These results highlight the scalability advantage of TATTOO, demonstrating its ability to leverage larger response pools more effectively than existing PRMs.

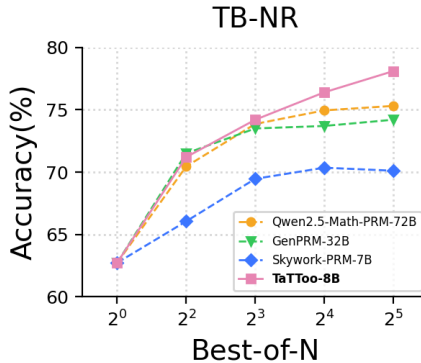


Figure 8: Performance of TATTOO and baseline PRMs on TB-NR under Best-of-N test time scaling. While baseline models plateau as N increases, TATTOO continues to scale effectively, yielding consistent accuracy gains.

H LIMITATIONS AND BROADER IMPACTS

While reinforcement learning with reward shaping enhances our PRM’s ability to capture fine-grained tabular reasoning signals, it introduces more computational overhead. Compared to SFT-only training, the RL stage requires additional rollouts, reward evaluations, and optimization steps, which can increase training cost and resource demands. This overhead may hinder reproducibility and accessibility in low-resource environments, motivating future work on more efficient reward objectives and lightweight reward modeling strategies. In addition, our current framework is limited to text-table reasoning, and extending it to multimodal settings (e.g., integrating charts or image-based tables) remains an important direction for future work.

From a broader perspective, this work highlights the potential for process reward models to enhance structured reasoning in domains such as fact-checking, scientific analysis, and decision support. At the same time, reliance on automated verification carries risks: if tools or training data contain errors, these may be amplified rather than corrected. We encourage future research to explore mechanisms for auditing verifier reliability, reducing the energy footprint of RL training, and ensuring equitable performance across diverse application domains.

1296 I TATTOO ON STRONGER POLICY MODELS

1298 To further validate TaTToo, we evaluate our method using three strong downstream policy models:
 1299 Qwen3-32B (thinking mode) (Yang et al., 2025a), Qwen3-30B-A3B (thinking mode) (Yang et al.,
 1300 2025a), and gpt-oss-20b (Agarwal et al., 2025). We utilize the same Best-of-N Test-Time Selection
 1301 (TTS) setup described in section 5. We compare TaTToo against three strong baselines: Skywork-
 1302 PRM (He et al., 2024a), the Qwen-PRM series (Zhang et al., 2025b), and GenPRM (Zhao et al.,
 1303 2025), and evaluate performance on the TB-DA (Wu et al., 2024), WTQ (Pasupat and Liang, 2015b),
 1304 and MMQA (Wu et al., 2025a) tasks. The results are detailed in Tables 6, 7, and 8.

1305 Across all three stronger policy models, incorporating TaTToo consistently leads to better downstream
 1306 performance compared with larger-size baseline PRMs. This aligns with our observations in section 5
 1307 and further demonstrates TaTToo’s supervision effectiveness across policy models of varying sizes.

1309 Table 6: Main results of TATTOO on 3 different tabular reasoning tasks. We report the best-of-N
 1310 (with $N = \{4, 8, 16, 32\}$) performance using **Qwen32B (thinking)** as the policy model and compare
 1311 against various step verifiers. The best and second-best results are highlighted.

Verifier (Best-of-N)	Params	TB-DA				WTQ				MMQA			
		4	8	16	32	4	8	16	32	4	8	16	32
Skywork-PRM-7B	7B	34.6	35.8	35.6	35.3	78.5	80.1	81.4	81.9	37.2	38.6	39.1	39.4
GenPRM	32B	38.1	38.5	39.2	38.7	81.2	82.9	84.0	84.6	39.4	40.5	41.8	42.7
Qwen2.5-Math-PRM-72B	72B	37.4	38.3	39.4	39.1	82.3	84.2	86.1	86.7	42.2	43.8	44.2	44.8
TATTOO	8B	38.3	39.5	40.5	41.3	83.8	86.5	87.3	88.6	41.7	43.8	44.7	46.3

1320 Table 7: Main results of TATTOO on 3 different tabular reasoning tasks. We report the best-of-N
 1321 (with $N = \{4, 8, 16, 32\}$) performance using **Qwen3-30B-A3B (thinking)** as the policy model and compare
 1322 against various step verifiers. The best and second-best results are highlighted.

Verifier (Best-of-N)	Params	TB-DA				WTQ				MMQA			
		4	8	16	32	4	8	16	32	4	8	16	32
Skywork-PRM-7B	7B	29.4	31.1	31.9	32.2	70.2	72.0	73.9	75.0	29.4	30.9	32.0	33.1
GenPRM	32B	30.9	33.7	34.2	33.9	71.6	73.4	75.8	77.3	30.7	32.5	33.6	35.0
Qwen2.5-Math-PRM-72B	72B	34.8	35.3	35.6	37.2	72.5	74.6	77.1	78.9	31.9	33.8	35.0	36.5
TATTOO	8B	34.4	35.8	37.6	39.1	73.8	75.8	78.3	80.4	33.1	34.7	36.2	38.0

1331 Table 8: Main results of TATTOO on 3 different tabular reasoning tasks. We report the best-of-N
 1332 (with $N = \{4, 8, 16, 32\}$) performance using **gpt-oss-20b** as the policy model and compare against
 1333 various step verifiers. The best and second-best results are highlighted.

Verifier (Best-of-N)	Params	TB-DA				WTQ				MMQA			
		4	8	16	32	4	8	16	32	4	8	16	32
Skywork-PRM-7B	7B	27.2	28.3	27.9	28.1	71.0	72.8	74.2	74.5	33.4	38.1	38.5	38.8
GenPRM	32B	29.0	30.2	31.1	31.0	73.5	75.6	77.8	78.0	37.2	39.3	39.6	40.1
Qwen2.5-Math-PRM-72B	72B	33.1	34.7	34.9	35.5	74.2	76.5	78.7	79.3	39.5	40.5	43.4	43.9
TATTOO	8B	32.8	34.4	36.2	37.9	76.0	78.1	80.4	82.2	39.2	42.1	44.0	45.7

1350
1351 Table 9: Comparison of TaTToo with Output-Reward-Model (ORM) baselines.
1352
1353
1354
1355
1356

Method (Best-of-16)	TB-NR	TB-FC	TB-DA	WTQ	MMQA
Discriminative ORM	66.4	72.0	26.8	68.1	25.3
Generative ORM	70.6	75.9	28.5	69.2	26.6
TaTToo	76.4	81.2	33.6	73.5	29.1

1357
1358
1359 **J COMPARISON WITH ORM BASELINES**
1360

1361 To evaluate the efficacy of our approach, we compare TaTToo against two distinct Outcome Reward
1362 Model (ORM) baselines, both implemented on the same Qwen3-8B backbone. The comparison is
1363 reported in the table 9. We detail the training and implementation settings for these ORM baselines
1364 below. For the policy model and all additional configurations, we follow exactly the same setup
1365 as outlined in our main experiments. First, following (Mahan et al., 2024) and our established
1366 experimental settings, we employ a **Generative ORM** trained via a dual-stage process (SFT followed
1367 by RL) using our curated dataset. In this configuration, the model is optimized to generate a rationale
1368 chain before producing a final output-level reward token (“correct” or “incorrect”) for each complete
1369 instance. Second, adhering to the methodologies of (Hosseini et al., 2024; Cobbe et al., 2021), we
1370 implement a **Discriminative ORM** by training a classification head directly on the backbone model.
1371 This baseline is designed to classify whether a candidate answer’s final solution is correct or incorrect
1372 without generating any intermediate rationales.

1373 From the table 9, We can tell TaTToo provides significantly stronger supervision than both ORM
1374 baselines. This performance advantage indicates that TaTToo’s process-level supervision delivers
1375 denser and richer reward modeling signals, which in turn contribute positively to the performance
1376 of the downstream policy model. Furthermore, when comparing the two baselines, the Generative
1377 ORM consistently outperforms the Discriminative ORM. This gap suggests that the inclusion of
1378 generative rationales offers more informative supervision than binary correctness labels alone. Since
1379 the Generative ORM effectively leverages the reasoning paths within our training data, this result
1380 further highlights the rich verification rationales and high-quality supervision signals provided by our
1381 curated dataset.

1382
1383
1384
1385
1386
1387
1388
1389
1390
1391
1392
1393
1394
1395
1396
1397
1398
1399
1400
1401
1402
1403

1404 K COMPARISON WITH RAW QWEN3-8B AS A STEP-LEVEL VERIFIER

1405
1406
1407 Table 10: Comparison between TaTToo and a directly prompted Qwen3-8B verifier. TaTToo
1408
1409 consistently improves step-level supervision quality across all datasets.

1410 1411 1412 1413 1414 1415 1416 1417 1418 1419 1420 1421 1422 1423 1424 1425 1426 1427 1428 1429 1430 1431 1432 1433 1434 1435 1436 1437 1438 1439 1440 1441 1442 1443 1444 1445 1446 1447 1448 1449 1450 1451 1452 1453 1454 1455 1456 1457 Method	1404 TB-NR			1405 TB-FC			1406 TB-DA		
1407 4	1408 8	1409 16	1410 4	1411 8	1412 16	1413 4	1414 8	1415 16	
Raw Qwen3-8B	66.5	67.3	67.1	75.9	76.5	77.0	22.6	24.8	26.2
TaTToo (ours)	71.2	74.2	76.4	77.4	79.6	81.2	27.7	31.9	33.6

1404
1405
1406
1407
1408
1409
1410
1411
1412
1413
1414
1415
1416
1417
1418
1419
1420
1421
1422
1423
1424
1425
1426
1427
1428
1429
1430
1431
1432
1433
1434
1435
1436
1437
1438
1439
1440
1441
1442
1443
1444
1445
1446
1447
1448
1449
1450
1451
1452
1453
1454
1455
1456
1457
To isolate the effect of our curated training data and dual-stage training pipeline, we compare TaTToo with a baseline that directly prompts the raw Qwen3-8B model to act as a step-level verifier. The raw model receives the table, question, and full reasoning chain and is instructed to produce, for each step, a brief justification and a binary `correct/incorrect` label, matching TaTToo’s evaluation protocol. As shown in Table 10, TaTToo substantially outperforms this baseline, particularly on multi-step schema-interaction and tool-grounded cases, demonstrating that simply prompting a strong LRM is insufficient for reliable table verification. Instead, TaTToo’s curated dataset, schema-aware prefixing, and tool-grounded RL training yield significantly more accurate step-level supervision and consistently higher downstream performance under Best-of- N test-time scaling.

L INTEGRATING TATTOO WITH RL-TRAINED TABLE-R1

1404
1405
1406
1407 Table 11: Performance of Table-R1-Zero with and without TaTToo under the Best-of- N setting.
1408
1409 TaTToo consistently improves the RL-trained table reasoner across all tasks.

1410 1411 1412 1413 1414 1415 1416 1417 1418 1419 1420 1421 1422 1423 1424 1425 1426 1427 1428 1429 1430 1431 1432 1433 1434 1435 1436 1437 1438 1439 1440 1441 1442 1443 1444 1445 1446 1447 1448 1449 1450 1451 1452 1453 1454 1455 1456 1457 Method	1404 TB-NR	1405 TB-FC	1406 TB-DA	1407 WTQ	1408 MMQA
Table-R1-Zero	34.8	61.6	16.4	77.3	24.2
Table-R1-Zero + TaTToo (BoN-4)	39.6	64.7	18.3	80.9	26.8
Table-R1-Zero + TaTToo (BoN-8)	45.1	69.0	20.1	82.6	28.4
Table-R1-Zero + TaTToo (BoN-16)	48.2	72.3	23.5	84.5	30.3

1404
1405
1406
1407
1408
1409
1410
1411
1412
1413
1414
1415
1416
1417
1418
1419
1420
1421
1422
1423
1424
1425
1426
1427
1428
1429
1430
1431
1432
1433
1434
1435
1436
1437
1438
1439
1440
1441
1442
1443
1444
1445
1446
1447
1448
1449
1450
1451
1452
1453
1454
1455
1456
1457
To demonstrate that TaTToo is complementary to RL-based table-reasoning methods, we further evaluate its performance when paired with Table-R1-Zero (Yang et al., 2025b), a 7B table-specialist policy model trained with program-based reinforcement learning. Under the Best-of- N test-time sampling strategy ($N \in \{4, 8, 16\}$), we apply TaTToo as the verifier following the same evaluation protocol described in Section 5 and compare Table-R1-Zero alone against Table-R1-Zero augmented with TaTToo across all five tasks. As shown in Table 11, incorporating TaTToo consistently improves accuracy and yields larger gains as N increases, indicating that TaTToo reliably identifies higher-quality trajectories during test-time scaling. These results further confirm that TaTToo is architecture-agnostic and serves as a flexible verifier that enhances diverse table-reasoning systems, including RL-trained approaches such as Table-R1.

1458 M EFFECIENCY ANALYSES ON TATTOO
1459
14601461 Table 12: Computational cost breakdown of TaTToo training stages.
1462

TaTToo Training Stage	Training Data Size	# of Training Steps	GPU Setup	Total Hours	Total Cost
SFT	50K	~2400	8×A100	5.4	\$25.9
RL	10K	~280	8×A100	8.3	\$39.8

1466 To ensure computational efficiency, our design prioritizes concise data curation. As detailed in
1467 Section 4.2, we implement a progressive filtering strategy that yields a high-quality training set
1468 of approximately 60,000 examples. This dataset size is significantly more compact than standard
1469 Process Reward Model (PRM) corpora; for comparison, the baseline Qwen-PRM models utilized
1470 in our experiments required roughly 800,000 training samples (Lightman et al., 2023; Zhang et al.,
1471 2025b). Leveraging this compact dataset alongside a lightweight backbone allows the complete
1472 TaTToo training process to conclude in fewer than 8 GPU hours. Beyond efficiency, the resulting
1473 PRM demonstrates robust generalization capabilities. Once trained, TaTToo provides effective step-
1474 level supervision across a diverse spectrum of tabular reasoning tasks, including question answering,
1475 fact-checking, and data analysis, while still remaining compatible with various Test-Time Selection
1476 (TTS) strategies such as Best-of-N and Beam Search. This versatility underscores TaTToo’s broad
1477 applicability across the tabular reasoning domain.

1478 To quantify the accessibility of our method, we analyze the training overhead of TaTToo. We present
1479 a detailed cost breakdown for the 8B model, encompassing both the Supervised Fine-Tuning (SFT)
1480 and Reinforcement Learning (RL) stages. To provide a tangible economic metric, we evaluate the
1481 total GPU computational cost based on a standardized pricing rate of \$4.8 per 8-GPU hours.

1482 While the RL stage utilizes only approximately one-fifth of the data and one-ninth of the training
1483 steps relative to the SFT phase, it incurs a higher computational cost due to the overhead associated
1484 with rollout sampling and tool executions. However, the absolute duration of the RL stage remains
1485 limited. As demonstrated in Table 12, given the substantial performance improvements observed over
1486 the SFT-only baseline, this additional computational expenditure represents a favorable efficiency-
1487 effectiveness tradeoff. Overall, the complete TaTToo training pipeline requires approximately 14
1488 GPU hours, translating to a cost of roughly \$65. This resource requirement is considerably lower
1489 than that of training larger PRM baselines, such as those with 32B or 72B parameters.

1490
1491
1492
1493
1494
1495
1496
1497
1498
1499
1500
1501
1502
1503
1504
1505
1506
1507
1508
1509
1510
1511

1512

1513 **Case Study on TATTOO**

1514

1515 **(i) Before RL Training**

1516 Okay, I need to verify step by step for the provided answer and determine if each step is correct or not.

1517

1518 **[Step 0 Evaluation]**

1519 For step 0, let me first check whether it retrieves the correct information from the input table

1520 **[Step 3 Evaluation]**1521 Looking at step 3 and the table data provided, I need to verify whether the summarization calculation on the
1522 column "capacity in persons / hour" is correct. Let me add each part together:

1523

350 + 500 + 970 + 10000 + 2000 + 2800 + 650 + 650 + 1000 + 1000 + 720 + 820 + 1000 = **16,920**1524 (*wrong PRM calculation*)

1525

1526 Since the provided step 3 gives a final calculation result of 22,460, which is not equal to 16,920. Step 3 is
1527 incorrect due to the wrong summarization on the overall carrying capacity.

1528

The step is **\boxed{-1 (incorrect)}** (*X Wrong Step Reward*)

1529

1530

(ii) After RL Training

1531

1532 Alright, I am given a complete table, a question, and a corresponding answer. I need to check the correctness
1533 of each step of the answer. Let me verify step by step:

1534

[Step 0 Evaluation]

1535 I start by checking if Step 0 pulls the proper information from the table ...

1536

[Step 3 Evaluation]1537 To verify Step 3, I need to check the summarization (sum) over the "capacity in persons / hour" column. I will
1538 write Python code to verify this using the input table.

1539

1540

Code Sandbox

1541

1542

1543

1544

1545

1546

1547

1548

1549

1550

1551

1552

1553

1554

1555

1556

1557

1558

1559

1560

1561

1562

1563

1564

1565

```

table = {
    "columns": ["name or route", "capacity in persons / hour"],
    "data": [
        ["betten betten village", 350],
        ["betten village bettmeralp", 500],
        # ...
        ["trainerlift", 820],
        ["lager 1", 1000],
        # ...
    ],
}
capacity_index = table["columns"].index("capacity in persons / hour")
total_capacity = sum(row[capacity_index] for row in table["data"])

print("Total capacity in persons/hour: ", total_capacity)

```

Code Interpreter

Total capacity in persons/hour: 22460

Since the computed total of 22,460 aligns with the result in step 3, this step is correct.

The step is **\boxed{1 (correct)}** (*✓ Correct Step Reward*)Figure 9: **Case study on TATTOO before and after RL training.** Applying RL training enhances our PRM's dynamic utilization of tool calls, which in turn provides more reliable supervision over the input reasoning trajectories of LRM.